UNIVERSITÉ CATHOLIQUE DE LOUVAIN

ECOLE POLYTECHNIQUE DE LOUVAIN

TELE-LAB

Investigation of channel spatial diversity for dual-link cooperative communications in Wireless Body Area Networks

---

Supervisors
Luc Vandendorpe
Claude Oestges

Telecommunications
Master Thesis
Cristina Garcia

24th of August, 2010

Contents

Acknowledgment

I would like to thank some people without whom this thesis would not have been possible.

First of all, to my parents, since they always support me in the decision to make the thesis abroad and made it possible financially.

I would like to remark the attention provided by Claude Oestges and Luc Vanderdorpe when I was still in Barcelona, before coming to Louvain-la-Neuve, offering several projects and answering all questions kindly and quickly, as well as for their advice once I was here.

I would also like to acknowledge the technical support and patience of Lingfeng Liu and Vaibhav Bhatnagar, who helped me with every problem or doubt I had, always ready for discussing it and with new proposals when I got stuck. They also helped and accompanied me during all measurements that made this thesis possible.

Finally, I would like to appreciate the emotional support provided by Adrià Gusi and friends from Louvain-la-Neuve, who made my stay here become more than a Master Thesis, a unique experience that I will never forget.

Chapter 1

Introduction

In the last few years the interest of the Wireless Body Area Networks (WBANs) has been highly increased. These networks are based on compact wireless devices on, in and around the body that generally transmit in real time their measures to a common sink or coordinator. Recent technological advances in integrated circuits have enabled this devices to be miniature, lightweight, low power sensors endowed with the capacity to transmit and/or receive. When the data has reached the coordinator or base station it is possible for it to be sent on to devices via the internet for other to access.

The WBANs are a relatively modern invention and are primarily being designed to use within the health industry. Their main purpose is to permit doctors and other medical staff to safely monitor the health status of patients. One of the benefits of WBANs is that those patients with chronic diseases such as Alzheimer, Asthma and Diabetes can be monitored much more closely. Doctors will have the power to update patient records quickly and efficiently and they will be able to store information of the patient's general health.

This new type of technology hold much promise for future patient health monitoring. Moreover, the WBANs have attracted a growing interest not only for their loads of medical applications, but also for entertainment and wearable technology for fashion, as well as space and military applications.

1.1 Background

In this kind of networks, the propagation is affected by the limited communication range, the complicated spatial positions of the antennas and the scattering effect from the human body. The signal level randomly fluctuates, with some sharp declines of power known as fades. Since the noise variance

is usually constant, the instantaneous received Signal-to-Noise Ratio (SNR) fluctuates similarly to the channel energy s^2, and may drop dramatically during certain periods. When the channel is in a deep fade, a reliable decoding of the transmitted signal may not be possible, resulting in an error. This behavior is known as fading, and impacts the performance in terms of Bit Error Rate (BER) of any wireless system.

As an example, in an specific fading scenario, where the channel fading follows a Rayleigh distribution and a binary phase-shift keying (BPSK) modulation is used, the error rate may become affected decreasing only inversely with the SNR while the decrease of the error rate in non-fading Additive White Gaussian Noise (AWGN) channels is exponential with the SNR [1]. So, in a fading channel the BER performance will be worse than the one in an AWGN channel for the same SNR level.

In narrowband channels, the fading is defined as the time-variation of the channel path-loss, which is the attenuation term depending only on the distance R between the transmitter and the receiver. The time-variation of a transmission can be obtained measuring the channel through its transmission S-parameters by means of a Vector Network Analyzer (VNA). The fading is not further divided into fast and slow/shadow fading as little physical reason is found [2].

The time-variation of the propagation has tight connection with the body dynamics where the time-variant scattering effects from different parts of the dynamic body determine the patterns of the channel fading in time observation. For practical WBAN application architectures, the inclusion of body dynamics is necessary to gain the system performance.

To combat the impact of fading on the error rate, diversity techniques are usually employed. The principle of diversity is to provide the receiver with multiple versions of the same transmitted signal. Each of these versions is defined as a diversity branch. If these versions are affected by independent fading conditions, the probability that all branches are in a fade at the same time reduces dramatically. Hence, diversity helps stabilize the link through channel hardening which leads to improve performance in terms of error rate [1].

Because fading may take place in time, frequency and space, diversity techniques may similarly be exploited in each of these domains. As an example, time diversity can be obtained via appropriate coding and interleaving. Frequency diversity exploits the temporal spreading of the channel through equalization techniques [3] or multi-carrier modulations. Clearly, both time and frequency diversity techniques incur a loss in time or bandwidth to allow for the introduction of redundancy. By contrast, spatial or polarization diversity does not sacrifice time and bandwidth, since it is provided by the

use of multiple antennas at one or both sides of the link. This technique is also known as MIMO (Multiple-Input Multiple-Output).

Yet the spatial dimensions are increased by the use of antenna arrays. i.e. they are made of several closely-spaced antennas. The fading channel between each transmit-receive antenna pair can be modeled as a Single-Input Single-Output (SISO) channel. Yet each SISO channel constituting of the MIMO channel may be characterized by a different shadowing, which is the attenuation depending on the specific location of the transmitter and the receiver. Naturally, modeling only the individual SISO channels is not a complete representation of the multi-antenna channel behavior. Therefore, the statistical correlations between all matrix elements, which is the same that saying between all SISO channels, have to be characterized as well.

When there is no clear Line-of-sight (LOS) among the nodes located on different parts of the human body, or the movements of the body overshadow some node, diversity becomes an important solution. In order to provide more than one version of the information to the receiver, all transmitter antennas must have the same information to transmit. To accomplish this, relaying is an efficient and useful solution. Between the nodes and the destination there are placed some relays to make the wireless communication successful between them when the direct path suffers from a large attenuation as depicted in figure 1.1.

Relaying technique enhances the throughput of the system and provides more reliability towards errors. Simplifying, relays can be seen as repeaters, which repeat the information received from sending node and convey it to the destination. There are many applicable schemes available, which can be used at relays like: amplify and forward (AF), decode and forward (DF), etc, as described well in [4]. So, all the different diversity branches cooperate to provide reliable transmission and less risk of loosing information.

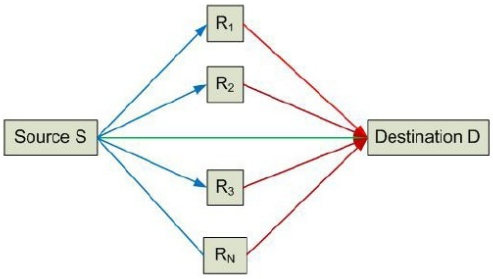

Figure 1.1: Relayed Network

1.2 Problem statement

Because of all the particularities mentioned before about WBANs, it is common to get high BERs in some of the links between the nodes situated on the human body. If there is a device which has non LOS (NLOS) with the receiver of its information (the coordinator) or the link suffers from high attenuation due to body movements, the fading will affect the transmission so that the information will arrive with errors. Since it is important not to lose any information due to the bad channel conditions or NLOS between the sending node and the central device, it is proposed in this project the use of relaying technique to provide a reliable transmission.

Moreover, Space-Time Block Code (STBC) is applied on relays to achieve a higher degree of robustness. STBC is a technique used in wireless communications to transmit multiple copies of a data stream across a number of antennas and to exploit the various received versions of the data to improve the reliability of data-transfer.

In this project the number of implemented relays is two (with the DF scheme), or which is the same that saying that the diversity order is two. So, the scheme is formed by two links working in cooperation to improve the BER performance. To implement the relaying technique a test bed is used. This test bed is the responsible of executing the transmission between the nodes which is set at the Industrial, Scientific and Medical band (ISM band), 2.45 GHz, because it is freely available and most practical existing technology for WBANs works in this band.

One of the goals of the project is to investigate the BER performance of the system when applying diversity and compare it with the simple case without relays, having a single transmission. So, the diversity benefits will be observed in terms of BER and SNR performance. To be able to compare them, dual transmission will be set so that each channel will have the half of the total transmission power that is used in a single-link transmission.

Another goal of the project is to analyze the channel statistics such as the temporal mean, the variance of each link, the power distribution that it best fits and the correlation of both links since, as mentioned before, it is significant for analyzing the whole MISO system. These measurements will be address by a VNA, which will provide the S-parameters of each channel. These results will depict how channel is affected by the body movements and it will be possible to compare this values with the BER performance measured by the test bed. There are also benefits of using diversity in terms of variance, they can be observed by the comparison of the variance of each single link with the one of the dual-link altogether.

Moreover, a relation between the correlation coefficients of both links and

both diversity benefits, in terms of BER and variance, will be attempted. Besides, a relation between how both benefits depend on each other will be procured. In order to compare the results obtained by the channel statistical analysis measured by the VNA and the ones related with the signal transmission procured by the test bed, the measurements will be done simultaneously. Each antenna from the VNA will be close to another one from the test bed. Summarizing the objectives are as follows:

- Investigate the BER performance for both the single and the dual-link and the channel diversity gain for each measurement.

- Analyze channel statistics.

- Study the benefits of using diversity in terms of variance.

- Compare results from the VNA measurements and the test bed's, such as channel statistics of different movements of the body with the BER performance.

- Trace a relation between diversity benefits and correlation coefficients between channels.

1.3 State of the art

This document marks almost eleven years from the first implementation of WBANs [5], though at that time, the prototype was named under Personal Area Network (PAN), a term that was originated from Zimmerman [6] and further developed by IEEE P802.15 Working Group [7]. Soon after, the notation of BAN emerged. A group from Philips was among the first to use BAN instead of PAN and has listed distinct features that should be incorporated into the two types of networks [8].

As the applications of PAN or BAN extended from connecting personal electronic consumer goods to medical and healthcare applications, BAN has become increasingly popular and is found to be a key element in the infrastructure for patient-centered medical applications [9]. The launch of projects, such as MobiHealth [10], further accelerates the development of BAN and m-Health service platform. IEEE T-ITB published a Special Section on m-Health six years ago [11] and the section turns out to be well recognized, as reflected in the number of citations.

Body area networks are not currently covered by existing communication standards. The IEEE 802.15 Task Group 6, IEEE 802.16.6, was formed to develop a communication standard optimized for low power devices and

operation on, in or around the human body to serve a variety of applications including medical, consumer electronics, personal entertainment and other. The channel modeling subgroup aims at proposing channel models for different configurations and band of BAN links [12]. The frequency bands proposed for the standard are: [13]

MedRadio: 401-402 MHz and 405-406 MHz for narrow band (less than 100kHz) and max. EIRP of -16dBm.

Medical Implant Communications Service (MICS): 402- 405 MHz for bandwidth less than 300kHz and max. EIRP of -16dBm. The communication is of type: Listen before talk (LBT)

ISM: 902-928MHz, 2.4 to 2.4835 GHz, 5.725 to 5.875 GHz, for bandwidth more than 500kHz and max. EIRP of +30dBm.

Wireless Medical Telemetry System (WMTS) frequencies: 608-614 MHz (bandwidth more than 1500kHz and max. EIRP of +10.8dBm), 1395-1400 MHz (max. EIRP of +22.2dBm), 1427-1429.5 MHz except at the locations listed in CFR Part 90.259(b)(4) where WMTS may operate in the 1429- 1431.5 MHz band (max. EIRP of +22.2dBm).

Ultra-WideBand: 3.1 to 4.9 GHz or 6 to 10.6 GHz.

In wireless communications in vicinity or inside of the human body, the channel depends largely on the body condition, activities, antenna position and the interaction associated between antenna and body as well as the local surrounding environment. Namely, the most significant difference of BAN from existing wireless networks is that the radio propagation channel necessarily includes the body effect, which plays an important role in radio propagation mechanism directly, and hence the channel is usually not stationary. Therefore the unique characteristics of the fading should be thoroughly investigated and efficiently modeled to design and develop the devices appropriately.

So far, a limited number of works have been made to characterize the on-body wireless channel with activity [14] - [20]. The measurements to capture the fading effect caused by activity have been conducted in various typical environments as well as in an anechoic chamber and found that the action is a primary factor for signal fading. To model this effect, dynamic narrowband on-body channel measurements mostly at ISM bands with custom equipments have been investigated in [15], [18], [19] and [20]; and in 4.5 GHz in [14]. Statistical analysis have been carried out and the results of significant statistical parameters including level crossing rate (LCR) and average fade duration (AFD) have been discussed in them. Moreover walking phantom

model was proposed to predict easily the mean and standard deviation values of the propagation channel of a walking subject [20].

Today, some works about cooperative mechanisms are addressed, like in [21] and [22], which describe different kind of cooperative mechanisms and they are compared by their Packet Error Probability (PER). However, this document try to focus on relaying techniques in practical scenarios, comparing the BER improvements with the time-variant channel measurements.

1.4 Outline

This document has been divided in 5 chapters. The first one has consisted on an introduction to better understand the aims of this project, a brief description of the state-of-the-art and how the project is structured. Chapter 2 explains in detail how measurements are set and all the instruments involved with them. In Chapter 3 the statistical analysis of the channels is developed from the VNA measurements results. Chapter 4 investigates the diversity benefits in terms of both BER and variance. Finally, Chapter 5 contains the final conclusions of the project and future work. Actually, there is also Chapter 6, which is composed of the Annexes, where there is the complete set of measurements results and all the figures that were not shown in the document because of spatial reasons.

Chapter 2

Measurement description

To carry out this set of measurements, two different devices have been used: VNA and a test bed developed by Vaibhav Bhatnagar that had been already used for another experiment of the same field. There are six antennas, three of them connected to the VNA and the other ones to the test bed. The ones connected to the test bed are going to be referred as antennas 1, 2 and 3 from now on. Antenna number 3 is the receiver and the other two the transmitters. The other three antennas, connected to the VNA, are referred as antennas 4, 5 and 6. In this case, antenna 4 is the transmitter and the other two the receivers. The antennas were placed on the body in a way that one antenna connected to the VNA is next to another connected to the test bed. So, the setup of the antennas for each part is shown in figures 2.1 and 2.2.

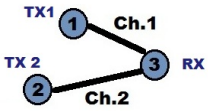

Figure 2.1: Setup of the antennas connected to the test bed

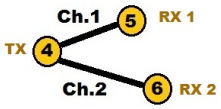

Figure 2.2: Setup of the antennas connected to the VNA

Although there are different number of transmitters and receivers in both parts, it doesn't represent a problem since by the principle of reciprocity it is known that a channel remains the same if the transmitter and receiver are switched. Besides, it is assumed that both devices are working under close channels, so that each measurement of a channel from the VNA can be matched with the same channel measurement from the test bed.

Each measurement is characterized by the arrangement of the antennas in the body (which is referred as scenario), the movement of the body and the

surrounding environment. In the following sections the measuring campaign is further explained, as well as all the elements that are involved.

2.1 Scenarios

Each scenario defines a different distribution of the antennas on the body. There are five scenarios, explained in detail in the following pages, and in each one of them channels are measured for each one of the body movements. In the figures that follow, the two channels formed by the antennas are shown.

To illustrate better both links they have been named as: Channel 1, characterized by the S_{21} parameter measured by the VNA, which corresponds to the channel from antenna A to the receiver antenna in the test bed; and Channel 2, related to the S_{31} parameter and transmission from antenna B to the receiver. Antennas colored by blue represent those connected to the test bed, and the yellow ones are the antennas connected to the VNA. The star drawn in the figures represents the navel. In the last scenario, antennas 1 & 5 and 2 & 6 are drawn in vertical to clarify the figure, but their polarization is the same as in the rest of scenarios.

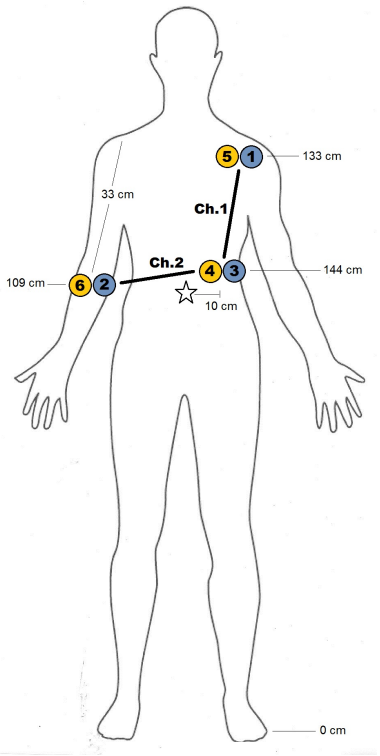

Figure 2.3: **Scenario 1,** in this scenario antenna 3 & 4 is on the left hip. One link is from the shoulders to the hip, so both nodes are more or less in a vertical line, while the other one is from the arm to the hip, where in case of walking one of the nodes will swing.

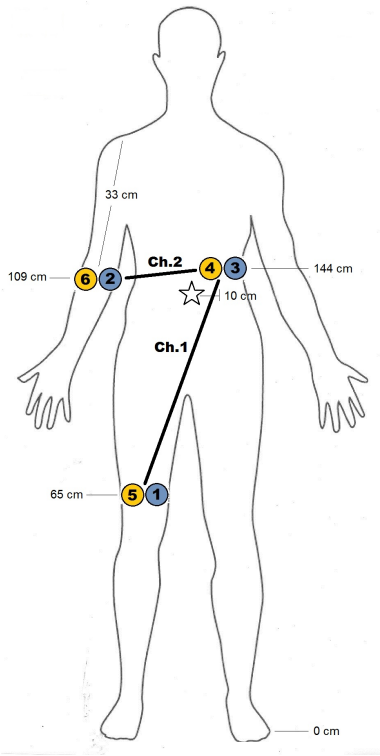

Figure 2.4: **Scenario 2,** in this case, antenna 3 & 4 remains in the same position that in scenario 1, as well as antenna 2 & 6. The other node is in the leg, so both links in the case of walking will have the nodes in parts that will be swinging.

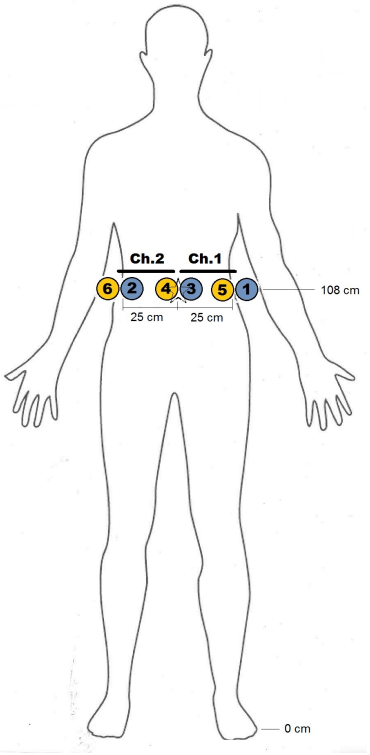

Figure 2.5: **Scenario 3,** this scenario set antenna 3 & 4 in the navel. Then, the other two nodes are symmetrically placed in each side, almost in the back part of the body.

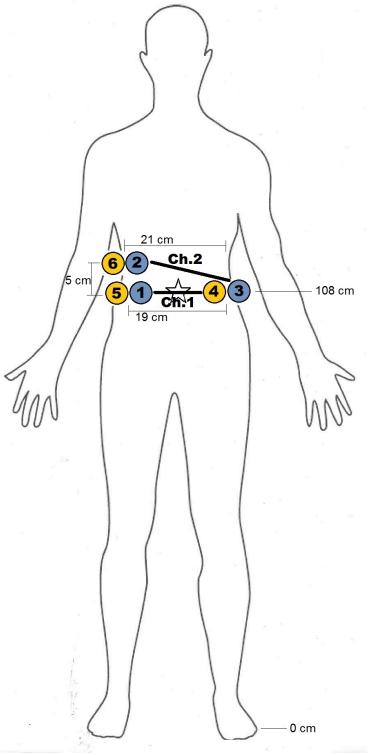

Figure 2.6: **Scenario 4,** in this case, antenna 3 & 4 is again placed in the left hip, but in the navel level. Both channels are similar here, separated by a small angle since node 2 & 6 is a little bit higher and further than node 1 & 5.

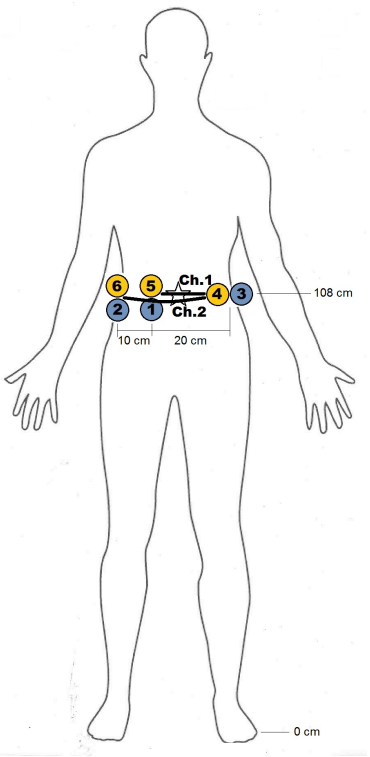

Figure 2.7: **Scenario 5,** this scenario keeps antenna 3 & 4 in the hip, with the other two antennas in the same horizontal line. Therefore, in this case channel 2 contains channel 1.

2.2 Body description

The antennas were placed on a female body, whose characteristics are described in the table 2.1. In order to ensure a repeatability of the measurements and a good subjection for the antennas, they are attached to the body by some elastic belts.

Height	170 cm
Weight	65 Kg
Waist radius	71 cm
Hip radius	88 cm

Table 2.1: Body characteristics

The target of this project are medical applications, so the movements of the body and the environments where the measurements took place try to reproduce some cases of interest in this field. Three different kind of movements are under study: *Laying on a bed*, *Stand-up/Sit-down/Stand-up* and *Walking*. The first two, considered as the dynamics ones, are measured in the laboratory where there are plenty of other instruments, tables and chairs. This way, it simulates a daily environment for people, with some objects that can cause reflections of the signal. On the other hand, a person laying on a bed, static, only breathing is measured, emulating a visit to the doctor or the fact of staying in a hospital.

The VNA and the test bed were on a cart, so that for the *Walking* case they could be able to follow the person while she was walking. Figures 2.8 and 2.9 depict the walking distance, approximately 3 meters. Figure 2.10 shows the *Stand-up/Sit-down/Stand-up* case and figure 2.11 the *Laying on a bed* one.

Figure 2.8: Walking case, start

Figure 2.9: Walking case, end

Figure 2.10: Stand-up/Sit-down/Stand-up case

Figure 2.11: Laying on a bed case

2.3 Antennas and cables

The six antennas used are the SMT-3TO10M-A model of SkyCross (figure 2.12), which is already the assembly including antenna element (13.6 x 16.0 x 3.0 mm), PCB (26.2 x 18.5 x 1.0 mm) and female SMA connector. Their frequency range is from 3.1 to 10 GHz, with a gain peak of 4.4 dBi at 4.5 GHz. They have a linear polarization and a radiation pattern of omni-directional azimuth.

Although the measured frequency is not in the effective range predefined, it shows still a good matching in VNA measurements when the antenna is mounted on the body. Antennas are vertically polarized and attached directly to the body, subjected by elastic belts.

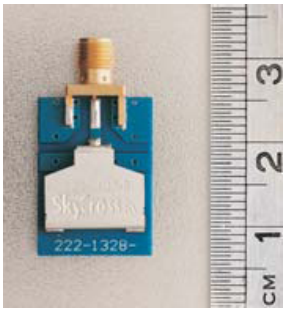

Figure 2.12: Antenna used

To connect the VNA's ports and the outputs of the test bed to the antennas, 6 coaxial cables are used. There are 5 cables of 4 meters and one of 8 meters. The first ones have an insertion loss of about - 1.8 dB and the other one of - 3.6 dB. The 8 meter cable is used to connect the receiver of the test bed.

2.4 Test bed

The test bed was used in this project to work with the signal transmission part. It was used before in another experiment and it was developed by Vaibhav Bhatnagar [23]. In that experiment was necessary to access the demodulated RF samples, so a hardware that allows this was needed. The hardware found is called USRP kit, shown in figure 2.13. It is an advanced digital signal processing (DSP) kit, which provides a flexible GNU radio environment for users to implement different MIMO networks.

Figure 2.13: USRP kit

Normally, a USRP kit associates one USRP motherboard that can accommodate more than one daughterboard at a time. Moreover, the number of daughterboards that USRP accommodates depends on specification of the daughterboard per the frequency of operation (2.45 GHz in our case). The USRP motherboard is a MIMO capable motherboard, which supports high speed mathematics for up and down conversion. It is a low cost board, which incorporates Analog to Digital (A/D) and Digital to Analog (D/A) converters, RF front-end (frequency translator), and Field Programmable Gate Array (FPGA). Normally it has 12 bit A/D converter and 14 bit D/A converter. It could digitize a 32 MHz baseband signal and can deal with 2 V peakpeak signal. The FPGA is mainly responsible for high speed mathematics, digital up conversion, and digital down conversion.

In general, there are plenty of daughterboards available in the market per the frequency of use, but the chosen one for that experiments was the RFX2400 daughterboard because it works as a transceiver. The frequency band for the RFX2400 is from 2.3 GHz to 2.9 GHz, similar to IEEE 802.15.4, the standard which the implementation of the test bed is based on. In our case, one USRP can accommodate maximum of two RFX2400 daughterboards at a time. Motherboard and daughterboard used are shown in figures 2.14 and 2.15.

Figure 2.14: USRP motherboard

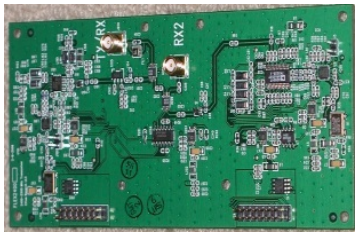

Figure 2.15: USRP daughterboard

The network considered for this report measurements is shown in figure 2.16. It consists only in two relays (R1 and R2) and one destination node (D). One of the relays may be the source and the other one is a node used to create the second link with two hopes, or both relays may be repeaters from another source node. In this implementation of the test bed, it is assumed that both relays have already received the same information from the rest of nodes or that they have already exchanged data and they have the same information to transmit, which means that the dotted line transmission is already done. This assumption helps to simplify the network, since the part of synchronization of the relays is not considered because is not a main goal of this project.

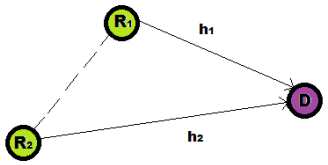

Figure 2.16: Wireless relayed network

Each node is accompanied by one Pentium III computer (Linux platform) and one USRP kit. All PC's must be connected to the local area network (LAN) because in order to satisfy the assumption that relays have the same information to transmit, it is necessary to perform a virtual network among them. For this implementation, the msocket matlab routine is used, which helps nodes to perform the virtual network and to exchange commands, acknowledgements and any other information needed during experiments. So, the software used for this experiment is mainly C++, Matlab and GNU radio. To know more about USRP kit and parts, the available technical report can be consulted [24].

The setup used for our experiment is shown in figure 2.17. There are two nodes: one acting as a master and the other one as a client. The client node is equal to the master, except for the USRP kit, which in the client's case has an extra daughterboard. The two daughterboards are necessary to implement the diversity in the transmission.

The test bed in this experiment uses an OFDM/4QAM modulation. Its parameters are shown in the table 2.2.

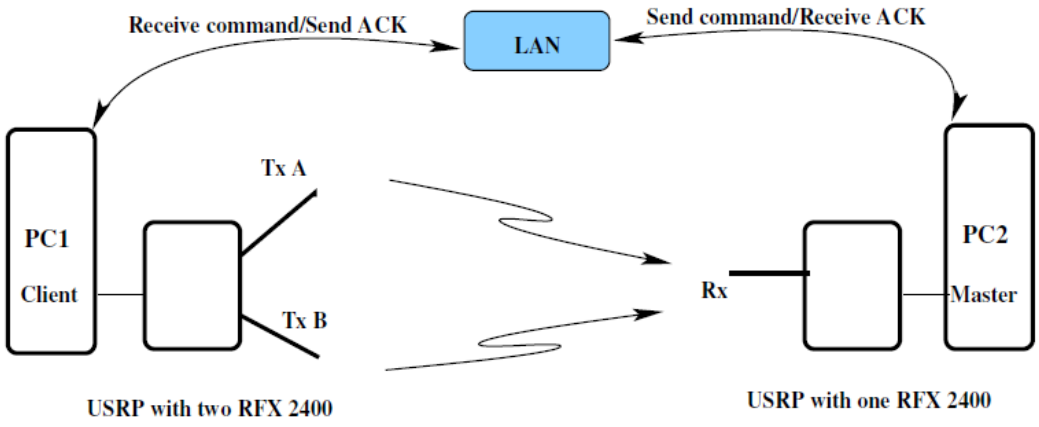

Figure 2.17: Setup of the test bed

FFT size	24
Length of cyclic-prefix	8
Number of symbols on burst	2
Number of bursts	24
Spacing between bursts	384
Sampling Frequency	4 MHz
Center Frequency	2.45 GHz
Signal Bandwith	20 MHz

Table 2.2: OFDM parameters

2.5 VNA

The VNA is used in this project to the channel measuring part. The model used at the laboratory is: Agilent PNA-X N5242A. Its key specifications are the followed ones:

- 10 MHz to 26.5 GHz
- 2- or 4-ports with two built-in sources
- 132 dB system and 130 dB receiver dynamic range, 32,001 points, 32 channels, 5 MHz IF bandwidth
- High output power (+18 dBm), low harmonics (-60 dBc) and a wide power sweep range (38 dB)
- Best dynamic accuracy: 0.1 dB compression with +13 dBm input power at the receiver
- Low noise floor of -114 dBm at 10 Hz IFBW

For more information, the data sheet and technical specifications can be found in [25]. The parameters used in the measurements with the VNA are shown in the table 2.3.

Narrowband	
Center Frequency	2.47 GHz
Transmission power	5 dBm
IF Bandwith	1KHz
Number of points	10001
Measurement time	10 s
Sampling Frequency	1 KHz
Ports	1,2 and 3

Table 2.3: VNA parameters

Chapter 3

Statistical Characterization of the channels

As was mentioned before, the two channels are measured through their transmission S-parameters, which are obtained with the VNA. In this section, the main statistics extracted from those S-parameters are presented: the temporal mean and variance of the channel power of each link is calculated firstly in linear scale and then converted to dB scale to be shown in figures. Besides, the correlation coefficients between the two links are also obtained. Further information about channels' statistics is provided in the Annex. Moreover, in order to characterize the measured channels, their power distribution is estimated.

Each movement was measured in each scenario twice (test 1 and test 2), so there will be 10 different measurements results for each one of the studied movements: *Laying on a bed*, *Stand-up/Sit-down/Stand-up* and *Walking*. In the figures, the first number refers to the scenario and the second one to the test. As an example, if the label is: 1.1, it refers to scenario 1, test 1. In addition, figure 3.1 recall all the scenarios to keep them on hand.

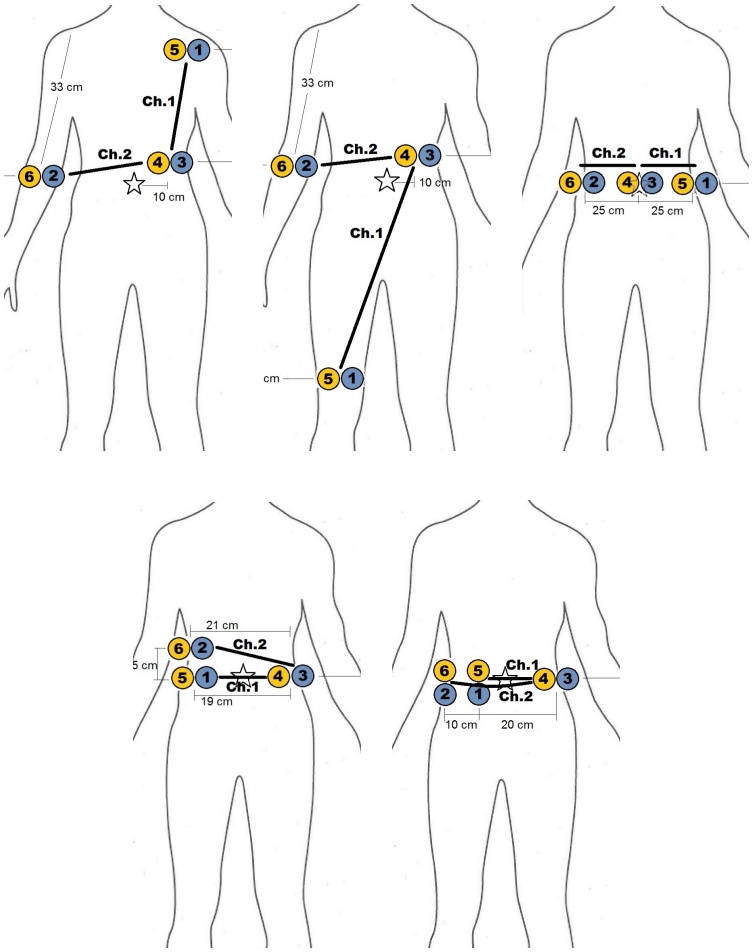

Figure 3.1: Summary of scenarios

3.1 Fading power temporal mean

Regarding the mean, in the *Laying on a bed* case it can be seen in figure 3.2 that in general all the channels in all scenarios suffer more or less the same attenuation. Both links, one characterized by the S_{21} parameter (channel 1) and the other one by S_{31} (channel 2), have in general similar values, except for the cases in scenario 3, where channel 1 is worse than channel 2 and in scenario 5, where channel 1 is better.

Taking into account that scenario 3 has both links symmetrical, this effect has to be caused by a different position of the left arm, covering the antennas more than the right arm does. In the case of scenario 5, where the transmitter is placed on the left hip and the other two antennas are in the same horizontal line but one further than the other, channel 1 is contained in channel 2. So, it makes sense that channel 2 has more attenuation than 1.

Moreover, when laying on a bed and inside a room with almost no furniture, the main propagation is due to creeping waves, which have to propagate along the abdomen, which is not normally a flat path. In addition to the fading power temporal mean values, the temporal behavior of the commented scenarios 3 and 5 can be seen in figures 3.3 and 3.4.

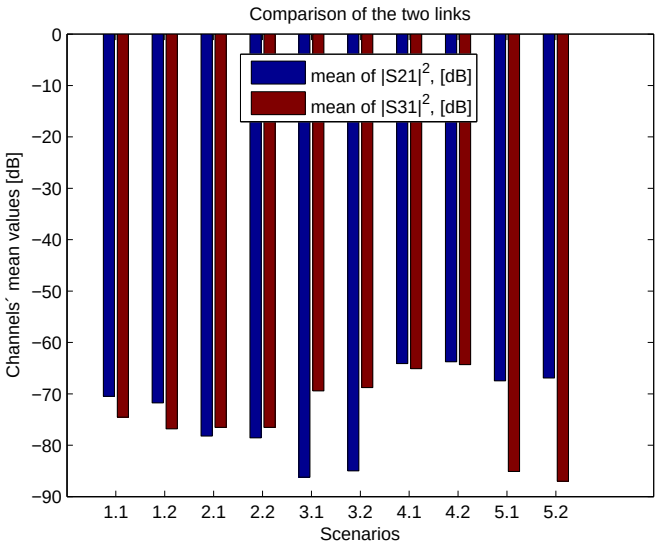

Figure 3.2: Mean value of the channels in each scenario, Laying

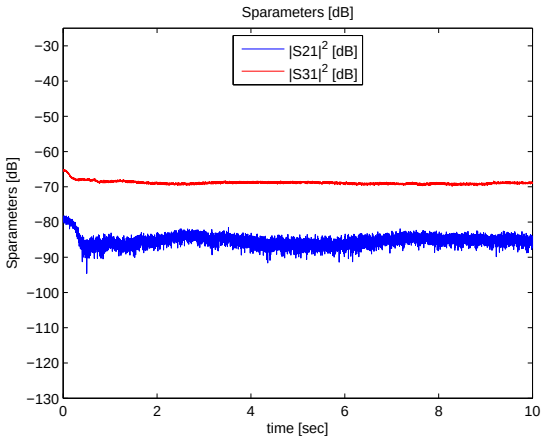

Figure 3.3: Channels values in dB scale for scenario 3, test 2, Laying

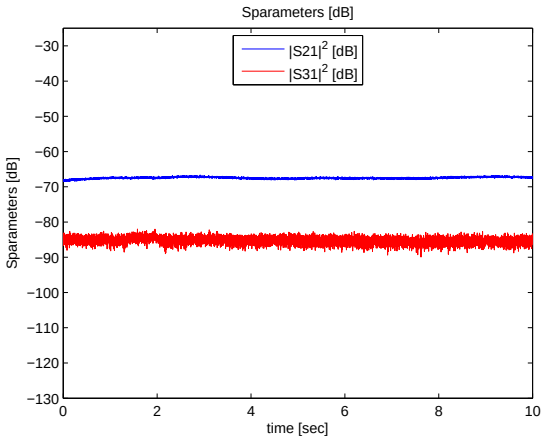

Figure 3.4: Channels values in dB scale for scenario 5, test 1, Laying

In the case of *Stand-up/Sit-down/Stand-up*, channels are also affected by the same attenuation (figure 3.5) in scenarios 2 and 3. However, in scenario 1, channel 1 is much better than channel 2. Moreover, channel 1 has less attenuation than any other channel among all scenarios. This can be because of the position of source antenna of channel 1, which is placed in the torso. When sitting down, the trunk is bent forwards, so the transmitter of channel 1 is closer to the destination placed on the hip of the same side of the body. In figure 3.6, it can be seen how the values of this channel keep constant during a period that can be attributed to the person while seated. At scenario 5 the behavior of the channel is similar to the case of *Laying on a bed* but with less difference of power between both channels during all transmission, as it can be seen in figure 3.7.

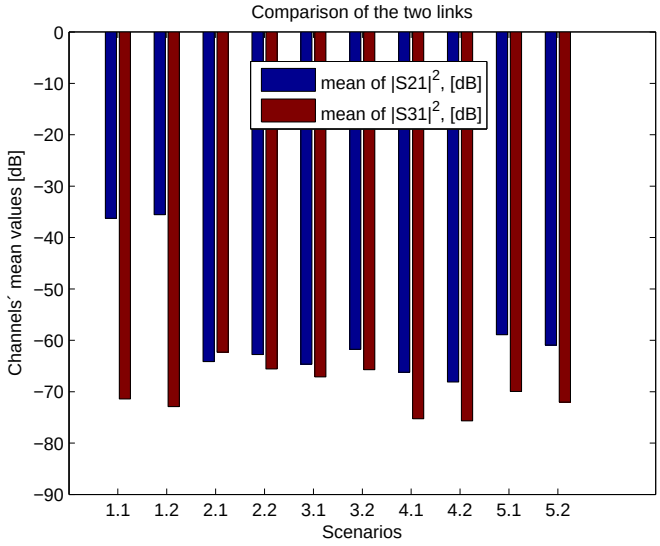

Figure 3.5: Mean value of the channels in each scenario, Stand/Sit/Stand

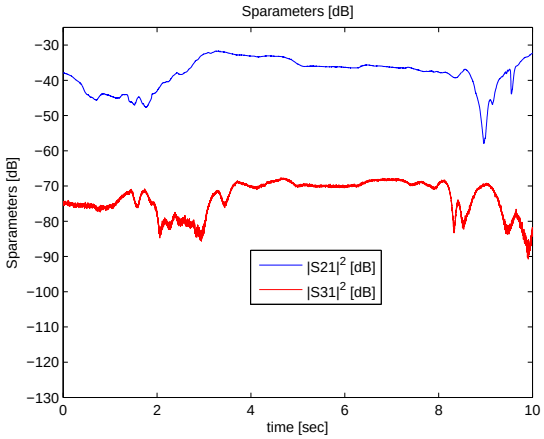

Figure 3.6: Channels values in dB scale for scenario 1, test 1, Stand/Sit/Stand

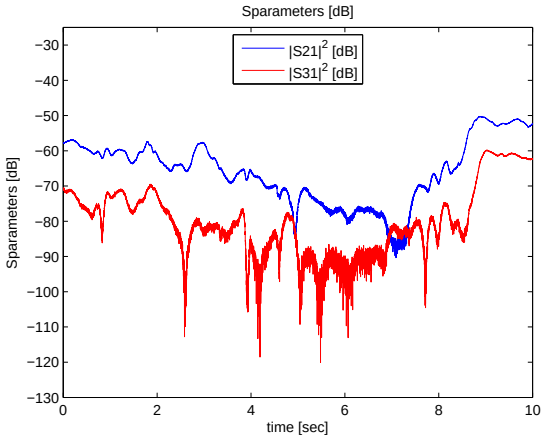

Figure 3.7: Channels values in dB scale for scenario 5, test 1, Stand/Sit/Stand

For the *Walking* case, also only scenario 2 and 3 have their channels with similar path-losses (figure 3.8). Scenario 3 has the receiver antennas placed symmetrically, so the arms movement while walking affects both channels in the same way; and in scenario 2 it is also understandable to have similar attenuation since both channels have their sources in extremities of the body that swing when walking (channel 1 on the leg, and channel 2 on the arm).

In scenario 1, channel 2 is much worse than 1. This can be due to the fact that in this scenario, channel 1 has its source and destination on the trunk and in the same side of the body, while channel 2 source is on an arm, which swings, in the opposite side of the destination. If the temporal behavior of the channel is observed, figure 3.9, channel 2 has more attenuation and it is more affected by the fading than channel 1. In scenarios 4 and 5, the source of channel 2 is further from the destination and closer to the arms than the source of channel 1. This causes a higher attenuation and deeper fading in some cases, as an example, figure 3.10 shows the particular case of how channels behaves during the measurements in scenario 4, test 1.

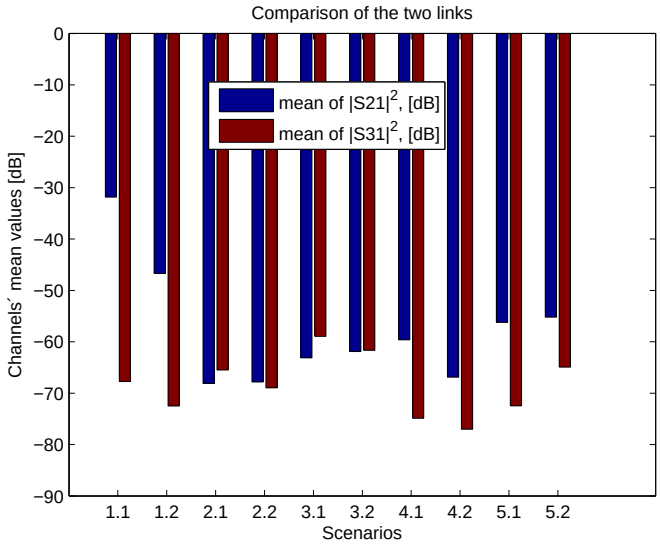

Figure 3.8: Mean value of the channels in each scenario, Walking

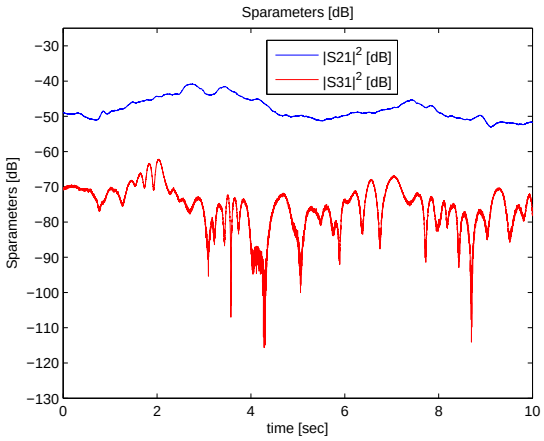

Figure 3.9: Channels values in dB scale for scenario 1, test 2, Walking

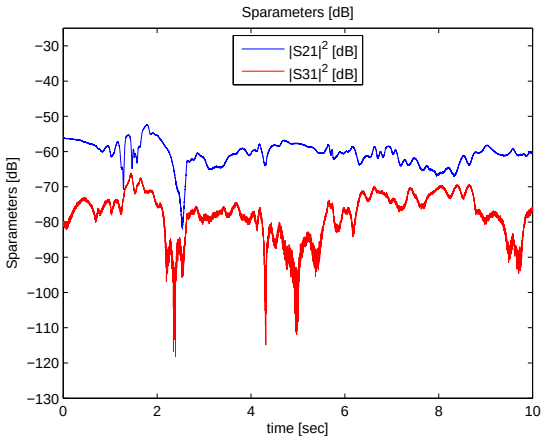

Figure 3.10: Channels values in dB scale for scenario 4, test 1, Walking

3.2 Fading power variance

The variance is also important to describe the behavior of the link, since it is a measure of the amount of variation within the values of the channel. The less variance a channel has, the more it behaves as a flat fading channel. In the following figures, variance is represented in dB scale to smooth the large differences between cases. Since the linear values of the variance were of order 10^{-15} for the *Laying on a bed* case and 10^{-12} for the dynamic cases, the dB values are negatives. Therefore, the closer to zero the value is, the higher is the variance of the channel.

With regard to the variance of the channels in *Laying on a bed* case, it depends on the scenarios. As it is depicted in figure 3.11, scenario 4 is the one whose channels have more variance. In that scenario $\sigma^2_{ch2} > \sigma^2_{ch1}$, as well as in scenario 2 and 3. So, in these scenarios, channel 1 is better channel than 2 in terms of variance. Unlike in scenario 1 where $\sigma^2_{ch1} >> \sigma^2_{ch2}$ or scenario 5 where the difference is larger.

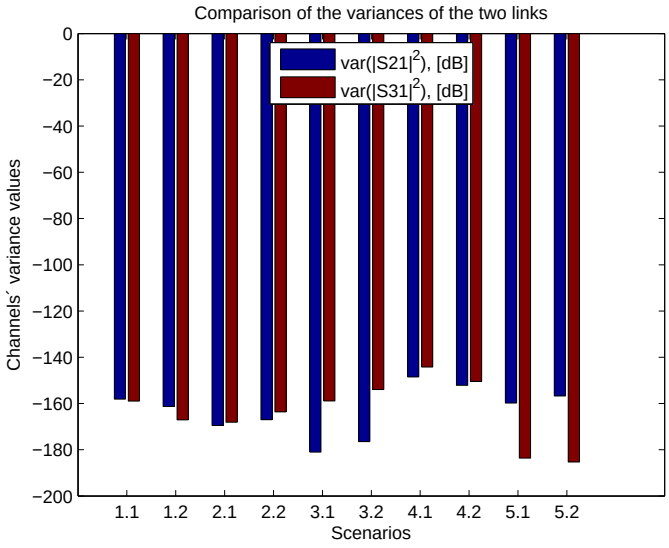

Figure 3.11: Variance of the channels in each scenario, Laying

In the *Stand-up/Sit-down/Stand-up* case (figure 3.12), in all scenarios except the second one, channel 1 has higher variance than 2, with greater differences in scenarios 1, 4 and 5. In scenario 2 one test has channel 1 as the worst channel and the other test, channel 2. So, it could be that both have similar variances.

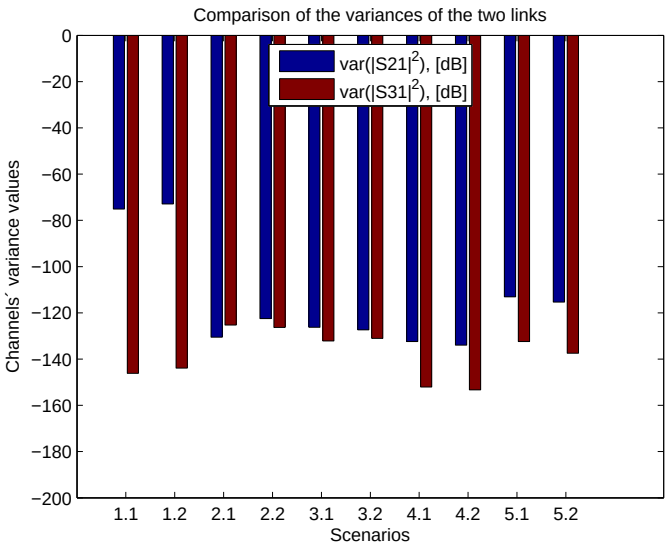

Figure 3.12: Variance of the channels in each scenario, Stand/Sit/Stand

For the *Walking* variances, as figure 3.13 shows, in scenarios 1, 4 and 5 $\sigma^2_{ch1} >> \sigma^2_{ch2}$, while in scenarios 2 and 3 the worse channel changes in each test, so they can be considered as if $\sigma^2_{ch1} \approx \sigma^2_{ch2}$.

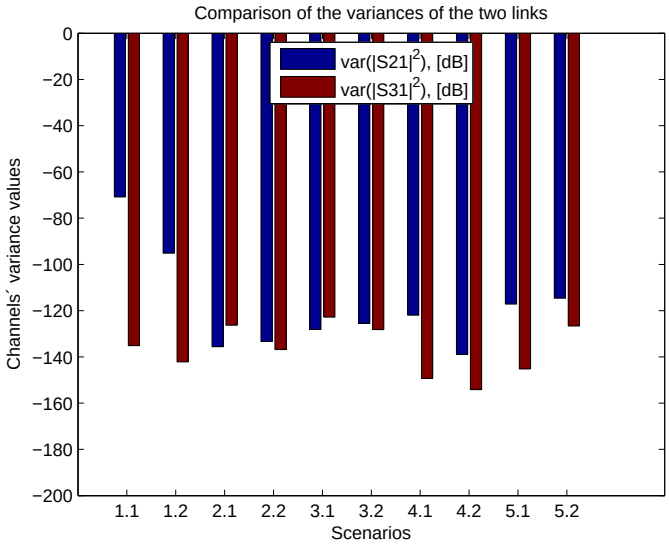

Figure 3.13: Variance of the channels in each scenario, Walking

3.3 Spatial channel fading correlation

Finally, the correlation coefficient between the two cooperative channels is also critical. The more correlated the channels (correlated channels are considered when $\rho \geq 0.7$), the less diversity benefit is achieved. Besides, if they are anticorrelated, the grade of diversity acquired can be larger. The correlation coefficients are calculated with Matlab, which uses the following formula:

$$\rho_{a,b} = \frac{C(a,b)}{\sqrt{C(a,a)C(b,b)}} = \frac{E\{(a-E\{a\})(b-E\{b\})\}}{\sqrt{E\{(a-E\{a\})^2\}E\{(b-E\{b\})^2\}}} =$$

$$= \frac{E\{ab\} - E\{a\}E\{b\}}{\sqrt{(E\{a^2\} - E^2\{a\})(E\{b^2\} - E^2\{b\})}}$$

where $C(a,b)$ is the covariance $\equiv Cov(a,b)$. If a and b are renamed for the cooperative channels, each one with half of the total power, $a = \frac{|h_1|^2}{2}$ and $b = \frac{|h_2|^2}{2}$, the correlation coefficient that Matlab uses is:

$$\rho_{\frac{|h_1|^2}{2},\frac{|h_2|^2}{2}} = \frac{E\{\frac{|h_1|^2}{2}\frac{|h21|^2}{2}\} - E\{\frac{|h_1|^2}{2}\}E\{\frac{|h_2|^2}{2}\}}{\sigma^2_{\frac{|h_1|^2}{2}}\sigma^2_{\frac{|h_2|^2}{2}}} \tag{3.1}$$

In the *Laying on a bed* case, channels are in general not correlated since they have such a smooth variation that it is difficult to ensure if they are similar or not in such little time. In the *Stand-up/Sit-down/Stand-up* case there is a measurement where channels are correlated, but the other ones are uncorrelated, so diversity benefits can be reached. As well as in *Walking* case, where moreover, there are some cases of anticorrelation, where a greater benefit can be achieved. These correlation coefficients of each movement can be seen in figures 3.14, 3.15 and 3.16.

This results can be compared with other correlation coefficients obtained in similar works about WBAN. In [15] a characterization of a time-variant WBAN channel is done. To accomplish this, some links set around the body are measured in an anechoic chamber and also indoors with some furniture; both with different kind of movements as being still, walking or running. Specifically, there are two measurements that could be compared with the ones under study in this project.

The channel with the transmitting antenna on the wrist and the receiver one on the chest can be matched with the scenario 1. The still case indoors can be compared with the *Laying on a bed* case: although in scenario 1 both tests have very different correlation coefficients in our measurements, the

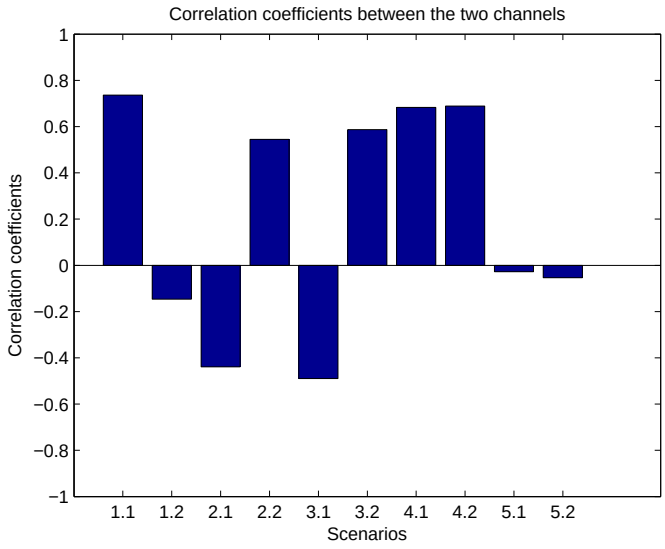

Figure 3.14: Correlation coefficients of the cooperative channels in each scenario, Laying

value obtained in the other report is similar to the test 2. About *Walking*, the result in the report is between the two possibilities obtained in our measurements in scenario 1. The other comparable channel is the one from the wrist to the thigh with the scenario 2. In the still position the values don't match as good as they do in the *Walking* case, which value is more or less the same than in the other report; *Laying on a bed* has uncorrelated and correlated values for the correlation coefficients while in the other report the value is between the two of them, with the channels uncorrelated.

In general, taking into account that measurements were done with different persons and different, but analogous, environments, it can be said that our results from the measurements are similar to that ones in [15].

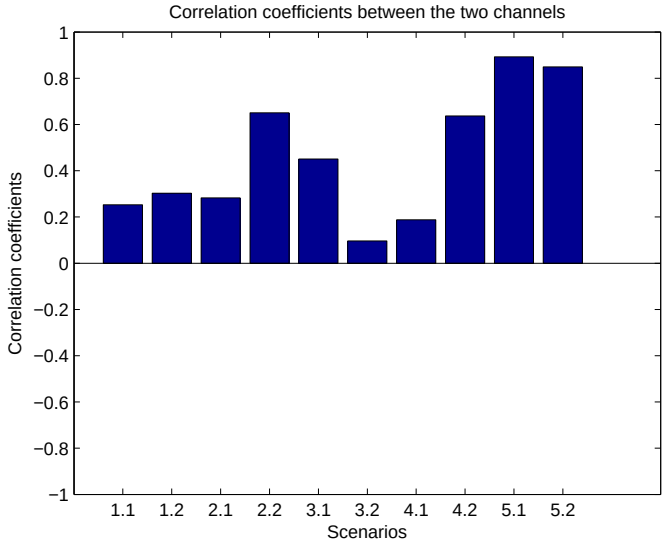

Figure 3.15: Correlation coefficients of the cooperative channels in each scenario, Stand/Sit/Stand

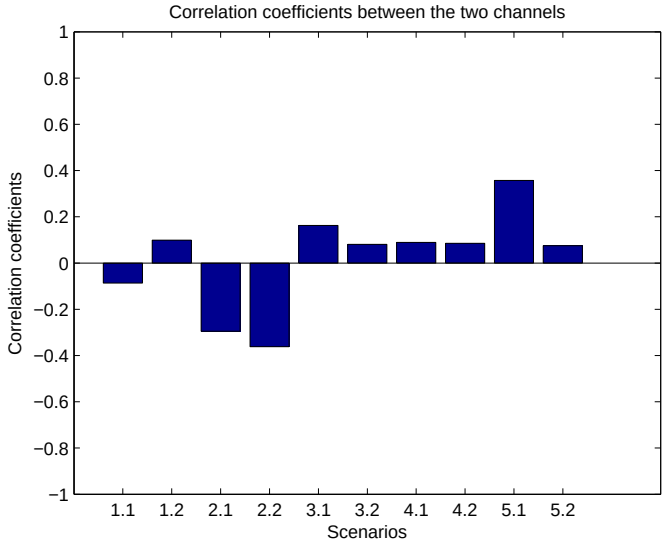

Figure 3.16: Correlation coefficients of the cooperative channels in each scenario, Walking

3.4 Fading power distribution

Besides the mean, variance and correlation coefficients study, a Probability Density Function (PDF) analysis is done. This is achieved by means of the estimation of the channel's Cumulative Distribution Function (CDF). With the values of the power of the channel, some CDF's of the main known distributions (Rice, Nakagami, Log-normal, Normal, Rayleigh, Exponential, Gamma, Weibull and Chi-square) are estimated by using the Maximum likelihood estimation (MLE) method. With that measured values of the channel is also calculated the empirical CDF. Then, this measured CDF is compared with each of the estimated CDF's to see which one of these estimations is the most similar to the empirical one. To decide it, Chi-square test is used:

$$\chi^2 = \sum \frac{(\hat{E}_i - E_i)^2}{E_i} \qquad I = 100,$$

where $\hat{E}_i$ is the estimated probability and E_i is the measured one, in each interval i of the observed data range. The lower value of χ^2 is, the best the estimated distribution fits with the measured one. So, in each one of the three movements under study the Chi-square test is done for both channels and the distribution that best fits each channel in the most part of the scenarios is chosen. For the following figures, the legend used to determine each distribution is depicted in figure 3.17.

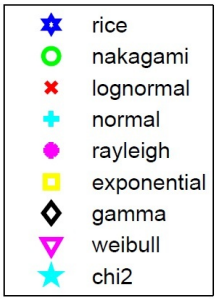

Figure 3.17: Legend for the Chi-square test

For the *Laying on a bed* case, channel 1 defined by the S-parameter $|S_{21}|^2$ follows the Normal distribution. Its averaged $\bar{\chi}^2 = 0.1231$ is very close to the value of the second distribution that better describes the channel, the Log-normal with a $\bar{\chi}^2 = 0.1318$. Channel 2 is better depicted by the Gamma distribution with a $\bar{\chi}^2 = 0.0031$, this time with a great difference from the second one, the Log-normal with a $\bar{\chi}^2 = 0.0242$. In figures 3.18 and 3.19 ,

the values of the Chi-square test for the $|S_{21}|^2$ and $|S_{31}|^2$ characterization are shown.

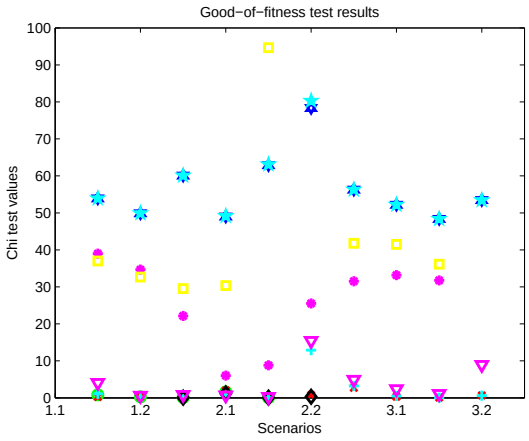

Figure 3.18: Good-of-fitness test results for channel 1, Laying

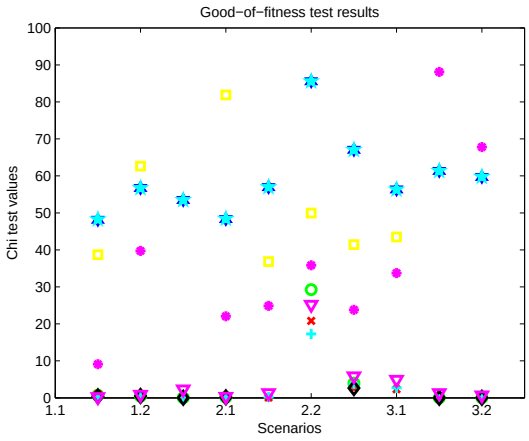

Figure 3.19: Good-of-fitness test results for channel 2, Laying

In the *Stand-up/Sit-down/Stand-up* case (figures 3.20 and 3.21), Gamma distribution represents in more scenarios the channel 1, however, it has in average a $\bar{\chi}^2 = 0.8538$, higher than other distributions such as Weibull or Exponential, whose $\bar{\chi}^2 = 0.2600$ and $\bar{\chi}^2 = 0.5330$, respectively. Channel 2 follows a Weibull distribution, $\bar{\chi}^2 = 0.2087$, with two other alternatives: Exponential and Gamma with $\bar{\chi}^2 = 0.6228$ and $\bar{\chi}^2 = 0.6485$.

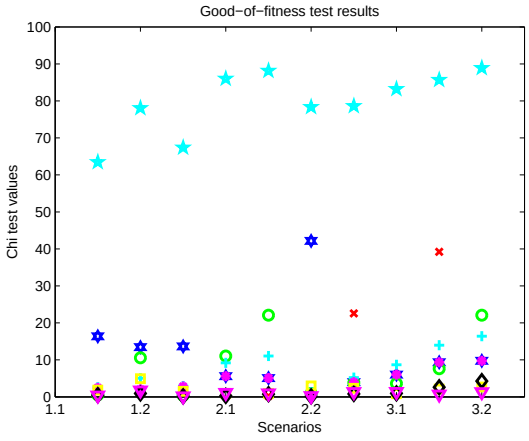

Figure 3.20: Good-of-fitness test results for channel 1, Stand/Sit/Stand

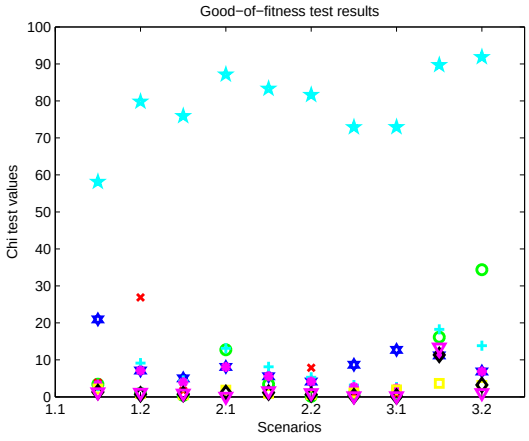

Figure 3.21: Good-of-fitness test results for channel 2, Stand/Sit/Stand

Finally, in the movement of *Walking* (figures 3.22 and 3.23), Gamma is also the distribution that in more scenarios represents better channel 1, but has a $\bar{\chi}^2 = 0.0311$, a little bit higher that the one of Log-normal distribution ($\bar{\chi}^2 = 0.0270$); Weibull distribution is also close to the Gamma value, $\bar{\chi}^2 = 0.0759$. For channel 2, Exponential distribution is the chosen one. It has a $\bar{\chi}^2 = 0.1214$, in comparison with the distributions that follow it closely: Gamma with $\bar{\chi}^2 = 0.1613$ and Weibull with $\bar{\chi}^2 = 0.2258$.

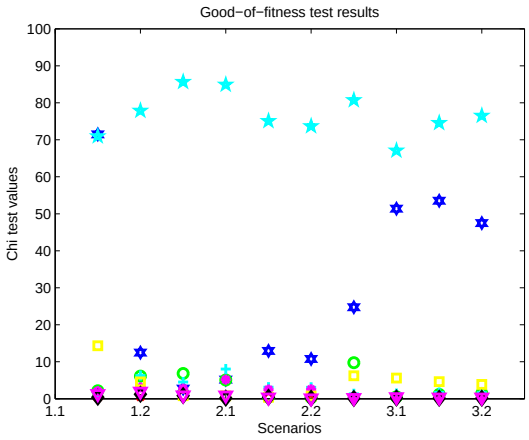

Figure 3.22: Good-of-fitness test results for channel 1, Walking

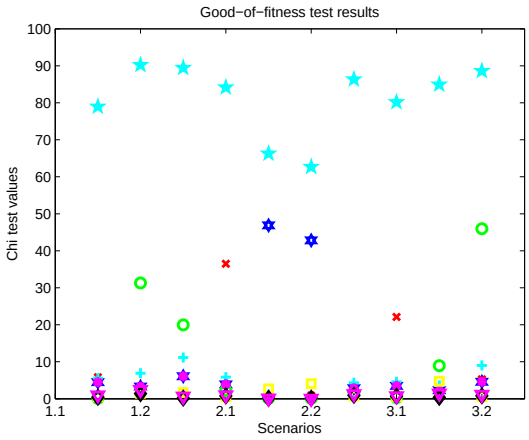

Figure 3.23: Good-of-fitness test results for channel 2, Walking

Table 3.1 summarizes all the cases.

Movements	**Channels**	**Distributions**
Laying on a bed	$\lvert S_{21}\rvert^2$	Normal (or Log-normal)
	$\lvert S_{31}\rvert^2$	Gamma
Stand-up/Sit-down/Stand-up	$\lvert S_{21}\rvert^2$	Gamma (also possible: Weibull or Exponential)
	$\lvert S_{31}\rvert^2$	Weibull (also possible: Exponential or Gamma)
Walking	$\lvert S_{21}\rvert^2$	Gamma (also possible: Log-normal or Weibull)
	$\lvert S_{31}\rvert^2$	Exponential (also possible: Gamma or Weibull)

Table 3.1: Estimation Distributions for each channel according to the three different movements under study

Chapter 4

Dual-link communication analysis

In this chapter, the cooperation scheme implemented by the test bed is explained in detail in order to get the formulas to study the system performance in terms of BER and analyze the advantages of using the cooperative channels instead of only a single transmission. Moreover, an analysis on the variance benefits of using diversity is done.

4.1 Cooperation scheme

In the signal part, an Alamouti code is used to apply the diversity in transmission. The same information is sent by the two antennas but in different time dimensions. At the same time, in order to achieve frequency diversity on top of space diversity, OFDM modulation is used. Therefore, OFDM has been combined with Alamouti coding. The symbols transmitted can be represented by table 4.1:

	Antenna A	Antenna B
Time t	$W^H x_1$	$W^H x_2$
Time t+T	$-W^H x_2^*$	$W^H x_1^*$

Table 4.1: Alamouti Code for two nodes

where W^H is the IFFT (Inverse Fast Fourier Transform) matrix (the first module in an OFDM modulation)[23], x_1 and x_2 represent the OFDM symbols, $x_1 = [x_{1,1} \dots x_{1,N}]^T$ and $x_2 = [x_{2,1} \dots x_{2,N}]^T$, where N is the number of subcarriers used during an OFDM symbol.

As it can be seen at the table, at time t antenna A sends the $W^H x_1$ symbol and antenna B the $W^H x_2$ symbol, whereas at time $t+T$ antenna A sends $-W^H x_2^*$ and antenna B $W^H x_1^*$. In this way, the receiver has two copies of the same symbol coming from different antennas, which exploit the transmit diversity. Therefore, signals received before the FFT can be seen as:

$$r(t) = r_t = H_A W^H x_1 + H_B W^H x_2 + n'_t$$

$$r(t+T) = r_{t+T} = -H_A W^H x_2^* + H_B W^H x_1^* + n'_{t+T}$$

where H_A and H_B are the circulant matrices of the channels between antenna A and the receiver and antenna B and the receiver. Besides, n'_t and n'_{t+T} are the receiver noises in each time slot.

After the FFT, the received signals become:

$$y_t = W r_t = W H_A W^H x_1 + W H_B W^H x_2 + W n'_t$$

$$y_{t+T} = W r_{t+T} = -W H_A W^H x_2^* + W H_B W^H x_1^* + W n'_{t+T}$$

where the noises can be renamed as: $n_t = W n'_t$ and $n_{t+T} = W n'_{t+T}$. Since H is circulant, WHW^H can be written as:

$$\Lambda = WHW^H$$

where Λ is the diagonal channel gain matrix for subcarriers from transmitter to the receiver. So, $\Lambda_A = W H_A W^H$, $\Lambda_B = W H_B W^H$. Then, the received signals are:

$$y_t = \Lambda_A x_1 + \Lambda_B x_2 + n_t$$

$$y_{t+T} = -\Lambda_A x_2^* + \Lambda_B x_1^* + n_{t+T}$$

The transmitted symbols, t_1 and t_2, can be recovered by means of the following linear operations:

$$t_1 = \Lambda_A^* y_t + \Lambda_B y_{t+T}^* = (|\Lambda_A|^2 + |\Lambda_B|^2) x_1 + \Lambda_A^* n_t + \Lambda_B^* n_{t+T}$$

$$t_2 = \Lambda_B^* y_t - \Lambda_A y_{t+T}^* = (|\Lambda_A|^2 + |\Lambda_B|^2) x_2 + \Lambda_B^* n_t + \Lambda_A^* n_{t+T}$$

With the help of zero forcing the symbols x_1 and x_2 can be extracted in the following manner:

$$\hat{x}_1 = (|\Lambda_A|^2 + |\Lambda_B|^2)^{-1} t_1$$

$$\hat{x}_2 = (|\Lambda_A|^2 + |\Lambda_B|^2)^{-1} t_2$$

and for the single link:

$$\hat{x} = \hat{\Lambda}^{-1} y$$

To estimate Λ_A and Λ_B a training sequence is used. As it can be seen in figure 4.1, each iteration of the transmission is formed by 24 burst with 2 OFDM symbols in each burst and 11 subcarriers in each OFDM symbol, and it takes 1.66 seconds. Normally, within the 10 seconds of the measurements the transmission contains six or seven iterations. The first OFDM symbol of each burst is used to send a known sequence. From that sequence the channel is estimated and then this estimation is used to recover the transmitted symbols from the second OFDM symbol. The calculation of the diagonal matrix of channels gains are:

$$diag(\hat{\Lambda}_A)_i = \frac{y_{A_i} x^*_{1_i} - y_{B_i} x^*_{2_i}}{x_{1_i} x^*_{1_i} + x_{2_i} x^*_{2_i}}$$

$$diag(\hat{\Lambda}_B)_i = \frac{y_{A_i} x^*_{2_i} - y_{B_i} x^*_{1_i}}{x_{1_i} x^*_{1_i} + x_{2_i} x^*_{2_i}}$$

where i means the i^th element of the symbol. In the single transmission case:

$$diag(\hat{\Lambda})_i = \frac{y_i}{x_i}$$

The symbols are estimated as mentioned before. The noise of the dual transmission can be estimated by:

$$\hat{n}_1 = \hat{\Lambda}^*_A y_t + \hat{\Lambda}^*_B y^*_{t+T} - (|\Lambda_A|^2 + |\Lambda_B|^2) x_1$$

and for the single antenna case:

$$\hat{n} = y - \hat{\Lambda} x$$

With the estimation of the channels and noises it is possible to obtain the SNR of each case:

$$SNR_S = \frac{\hat{\Lambda}^2}{\hat{n}^2}$$

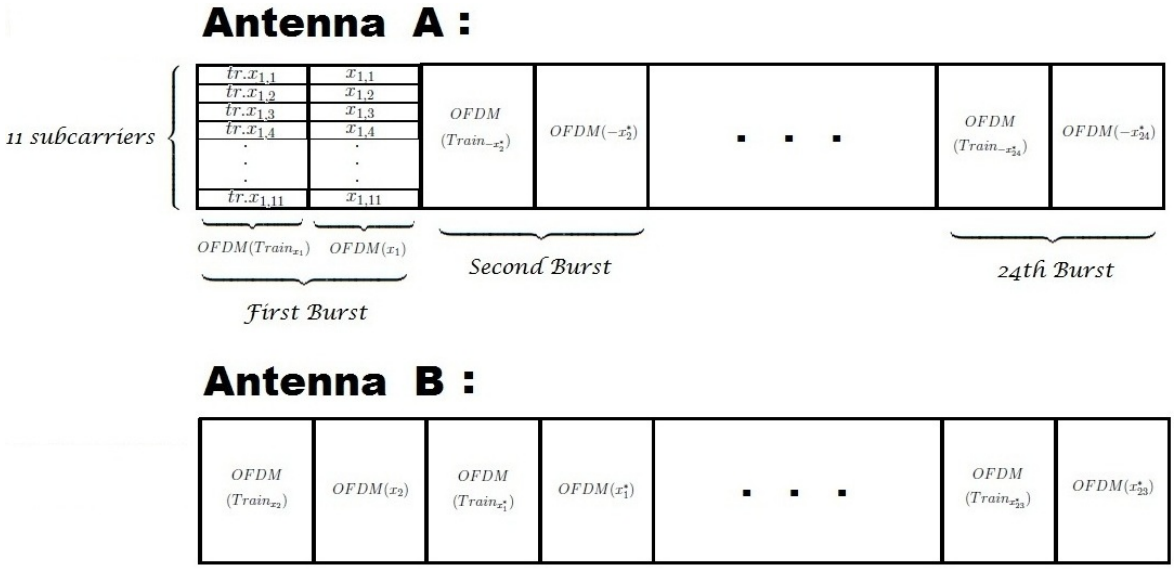

Figure 4.1: Structure of OFDM bursts

$$SNR_D = (\frac{|\hat{\Lambda}_A|^2 + |\hat{\Lambda}_B|^2}{\hat{n}_1})^2$$

To be able to compare both SNRs, the noise of the dual case $\hat{n}_1$ should be normalized by $\sqrt{|\Lambda_A|^2 + |\Lambda_B|^2}$. Then, the SNR is finally expressed as [27]:

$$SNR_D = \frac{|\hat{\Lambda}_A|^2 + |\hat{\Lambda}_B|^2}{\hat{n}^2} \quad (4.1)$$

where $\hat{n} = \frac{\hat{n}_1}{\sqrt{|\Lambda_A|^2+|\Lambda_B|^2}}$ is the normalized noise.

4.2 System performance based on BER

After some measurements it could be seen that, unfortunately, the SNR and BER results from the test bed were not satisfactory. In some iterations of the same measurement the BER and SNR achieved good marks with diversity but in other they didn't. By keeping two antennas (a transmitter and a receiver) close in the body surface without movement, it was proved that even in that short, LOS link in some cases low bit error rates were reached in the dual transmission while in other they were too high. This measurement was also done with dipole and monopole antennas, which were used for the test bed originally for the previous project. With them the measurement

achieved good marks with consistent results in all iterations. However, it was also observed that the test bed is unstable if it is kept on for a long time.

This could be due to a different radiation pattern between antennas used in this project and the test bed. The antenna matching was fine with the VNA but it seems these antennas are not suitable for the test bed because basically skycross works on 2.45GHz only on the body, otherwise it is designed for the frequencies over 3GHz. Moreover, the test bed is very sensitive for fera-body because body may absorb lots of transmitted power of signal and may disturb transmission.

Another reason could be that larger and faster phase change of the channel takes place with the current antennas. So, a separate measurement with both kind of antennas was made with the test bed to then determine the phase change in each case.

Antennas were placed in NLOS one from each other: the receiver was in the front part of the waist, near the navel while both transmitters were placed higher, symmetrically, almost in the underarm. The results (figures 4.2 and 4.3) showed that with the dipole antennas the phase changed slowly, with small increases between two consecutive symbols; while for the measurements with the antenna of this project, the SMT-3TO10M-A, the phase had abrupt changes from one symbol to the next one. This leads to a bad estimation of the channel in reception, which causes the low BERs provided by the test bed.

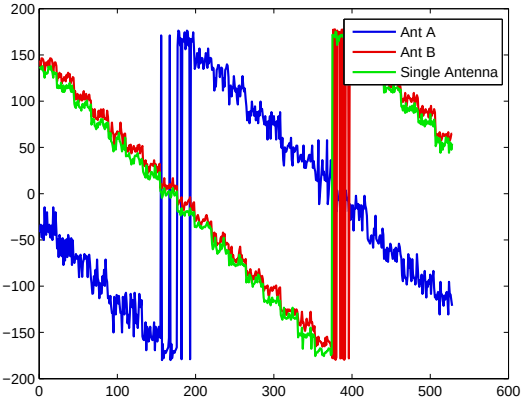

Figure 4.2: Phase change for the dipole antenna

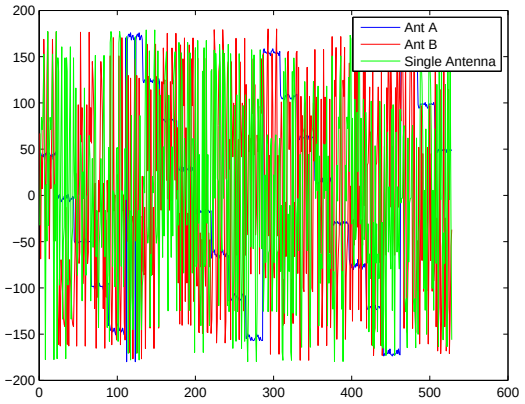

Figure 4.3: Phase change for the SMT-3TO10M-A antenna

The figures show a complete transmission of the test bed: 24 bursts with 2 OFDM symbols per burst and 11 subcarriers (with QAM constellation) per OFDM symbol, so 528 QAM symbols. Anyway, there is no need to take into account all 528 symbols, with the first 22 symbols is enough, since as explained before, in each burst the first 11 QAM symbols are associated to the training sequence and the other 11 to the information, and the following bursts do the same.

The coherence time, T_c, of a wireless channel is defined as the interval over which the channel $h_l[m]$ changes significantly as a function of m and it can be expressed as [27]:

$$T_c = \frac{1}{4\ D_s}$$

where D_s is the Doppler Spread, which is the largest difference between different Doppler shifts of all the paths that contribute to the transmission. This formula corresponds to a phase change of $\frac{\pi}{2}$, but if a phase change of $\frac{\pi}{4}$ is considered to be significant, the formula replaces the factor of 4 above by 8. In this report, it is used the second formula, which determines that a change of 45°during the T_c would lead to a bad estimation of the channel. In this project, the time interval where the phase change should not be abrupt is 22 symbols or multiples.

To illustrate a couple of cases, the phase change in scenario 1, test 1 and in scenario 2, test 1 have been calculated, both in the *Walking* case. In addition, a zoomed figure of the dipole antenna case is shown. It can be seen in the legend these figures that the test bed uses antenna B for the single transmissions, while in this document the single link has been presented as that one characterize by the S_{21} parameter, so it should be antenna A of the test bed. This was a mistake because the two daughterboards were mislabeled. However, since the results from the test bed are not being used, this does not affect any other part of the document. Both figures are zoomed in the first 22 symbols, with the margins within which the phase should remain (phase of the first symbol ± 45°).

It can be seen in figure 4.4 that antenna A, related to the channel characterized by S_{21} parameter, has an acceptable phase change, but antenna B, characterized by S_{31} parameter, has large changes of its phase. This results in a good BER performance in almost all iterations for the combination of the two links, while the single BER is worse than it should be because of the phase problems. So, the diversity benefit will not be only due to the benefits of the combination of two links, but for the bad estimation in the single link.

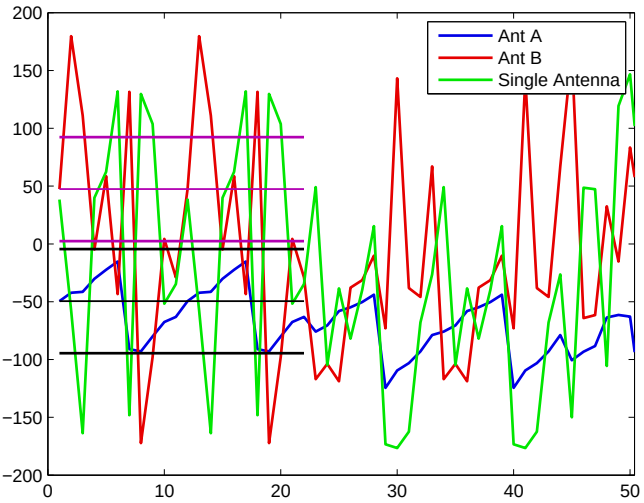

Figure 4.4: Phase change with the SMT-3TO10M-A antenna in scenario 1, test 1, Walking

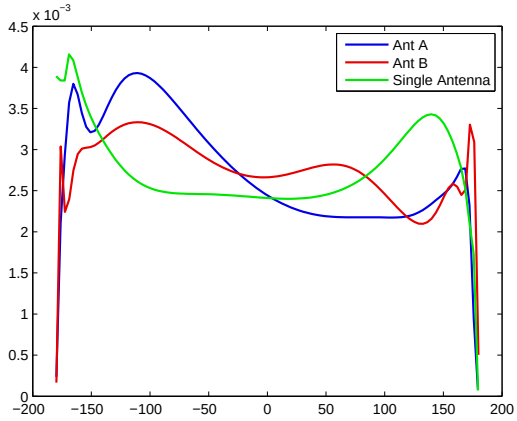

Figure 4.5: PDF of the phase change for the SMT-3TO10M-A antenna in scenario 1, test 1, Walking

Regarding the other case, in figure 4.6 it can be seen that both antennas suffer from large phase leaps, so the BER performance is poor in both single and dual transmissions. In figure 4.8 there is a zoom of the dipole antenna case, where it can be better appreciated that phase change for both transmissions is acceptable, so there is a good estimation of the channel. For each one of these cases, the PDF of the phase is also shown to better compare them.

If the phase change is analyze for all the scenarios and tests, it can be observed that when an antenna introduces a large phase change coincides when that channel suffers from a high path-loss. Therefore, both reasons may be right since the different radiation pattern between antennas and the test bed may be the cause of the large and fast phase change.

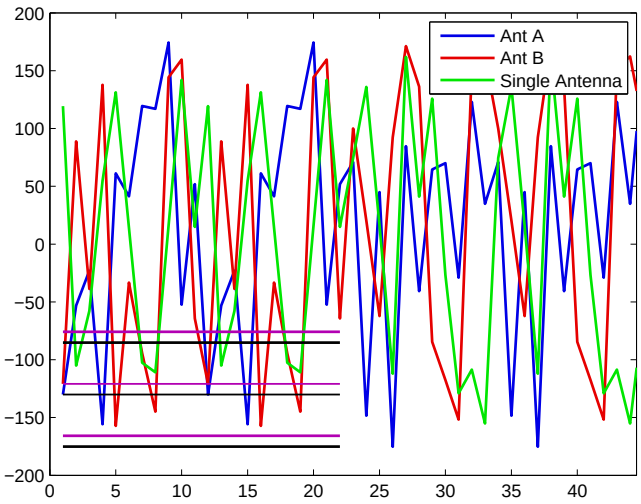

Figure 4.6: Phase change with the SMT-3TO10M-A antenna in scenario 2, test 1, Walking

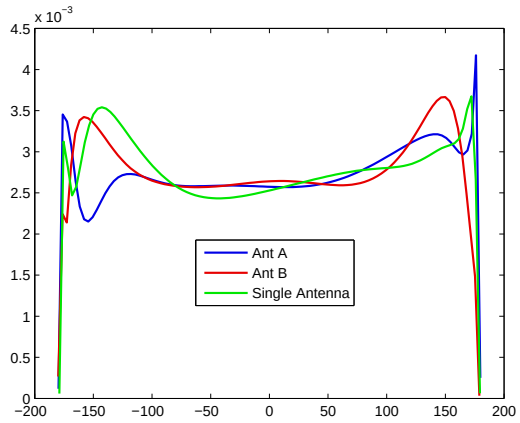

Figure 4.7: PDF of the phase change for the SMT-3TO10M-A antenna in scenario 2, test 1, Walking

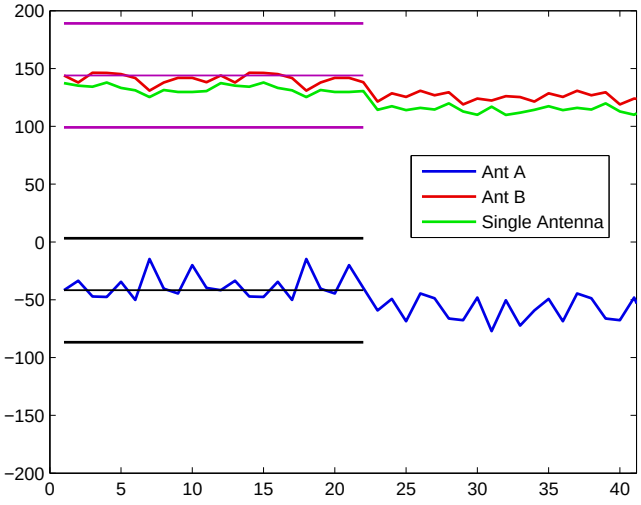

Figure 4.8: Zoomed phase change for the dipole antenna

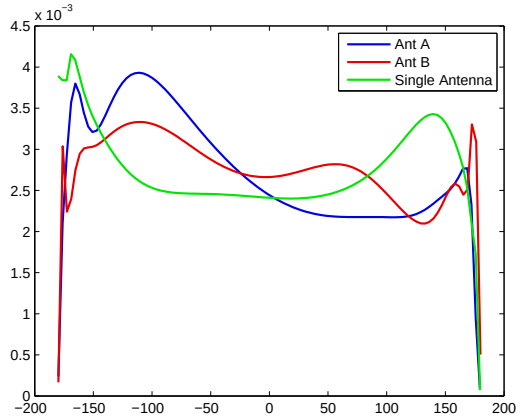

Figure 4.9: PDF of the phase change for the dipole antenna

Since the results from the test bed can not be used for lack of consistence, the BER benefits of using diversity are approached by the S-parameters measured with the VNA. However, BER is going to be calculated keeping in mind that the modulation that would be used for this scheme if the test bed would be used is a 4QAM or QPSK.

In absence of fading, the bit error rate in an additive white Gaussian noise (AWGN) channel can be calculated by:

$$BER = Q(\sqrt{\frac{2E_b}{N_0}}) = Q(\sqrt{2SNR_{Tx}})$$

When fading is considered, the received signal level fluctuates, so a new variable $\gamma_b = s^2 \cdot SNR_{Tx} = SNR_{Rx}$ is created, where s represents the channel fading, measured by the S-parameters with the VNA. As a result, the bit error rate has to be obtained by averaging the error probability for a fixed amplitude s over the entire range of s:

$$BER(SNR_{Tx}) \quad = \quad \int_0^\infty Pe(SNR_{Rx}) p(SNR_{Rx})\, dSNR_{Rx} \tag{4.2}$$

where SNR_{Rx} is the signal-to-noise ratio with fading for a particular value of s, $Pe(SNR_{Rx})$ is the bit error probability conditioned on a fixed SNR_{Rx}, $p(SNR_{Rx})$ is the probability density function of SNR_{Rx}, and $BER(SNR_{Tx})$ is the averaged bit error probability.

Since the data is discrete, 4.2 can be simplify as:

$$BER \quad = \quad \sum_{n=1}^{K} \frac{Q(\sqrt{2 \cdot SNR_{Rx}})}{K} = \sum_{n=1}^{K} \frac{Q(\sqrt{2 \cdot s^2 \cdot SNR_{tx}})}{K} \tag{4.3}$$

where K is the number of samples of the S-parameter.

Since the main aim of this project are the diversity gain results, the mean of the channels should be removed to separate the diversity performance from the channel gain. So, the channels were normalized by removing their mean in dB scale and adding a common reference level for both channels. Then, in linear scale again, the SNR_{Rx} was calculated to obtain the BER for the normalized channels.

By the BER performance, the benefit of using cooperative channels can be approached. The increase in the error rate slope as a function of the SNR determines the improvement by applying spatial diversity in the system. An example is shown in figures 4.10 and 4.11 (with BER represented in log scale), where the cooperative link has better bit error rate than the added link, but worse than the single one. This is because, as it was mentioned before, the

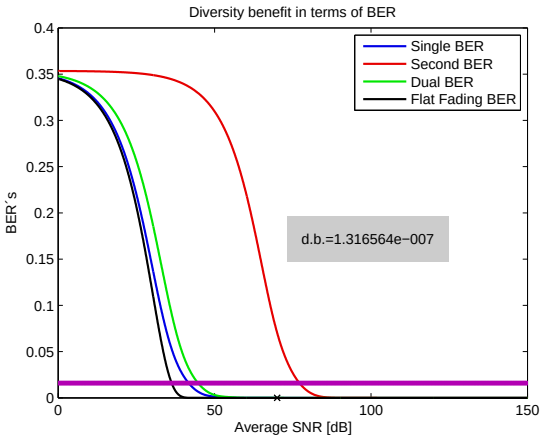

Figure 4.10: BER curves for the scenario 1 test 1, Stand/Sit/Stand

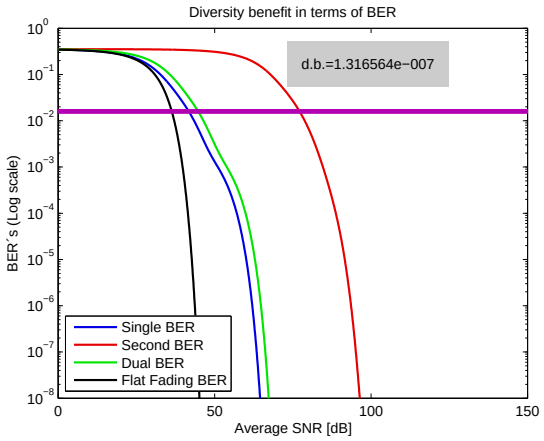

Figure 4.11: BER curves for the scenario 1 test 1, Stand/Sit/Stand in log scale

channel benefits from a channel gain and a diversity gain. The first one is related with the channel mean, so it is relative to each link.

After removing the mean, the increment in the slope is only due to diversity gain. It can be seen in figures 4.12 and 4.13 that, with the same example as before, diversity benefit exists: the BER curve of the dual link is always under the other two.

In these figures there is also plotted a flat fading channel as a reference. Among the different kind of fading channels the flat fading has a better BER performance because its power remains constant during the transmission.

Since these curves are being calculated from the S-parameters rather than SNRs extracted from the test bed, the real SNRs of the transmissions are unknown. Nevertheless, in order to determine a BER benefit of using diversity, an specific SNR is need to compare the curves. This concrete SNR is chosen within an area of valid SNRs for our experiment. This area was compute based on the fact that a deep fade occurs when $s^2 \cdot SNR_{Tx} = SNR_{Rx} \leq 1$, where s represents the fading [27]. Therefore, to ensure a good performance $s^2 \cdot SNR_{Tx} = SNR_{Rx} \geq 1$ has to fulfilled. So, $Q(\sqrt{2 \cdot SNR_{Rx}}) \leq Q(\sqrt{2})$, which implies:

$$BER \leq 0.0161$$

From this result, the SNR_{Tx} chosen to determine the BER benefit must be in that range. For the figures with no normalized channels it has been chosen 70 dB, and for the normalized cases is 4 dB. This decision is to illustrate some specific results and these two points have been selected so that in the

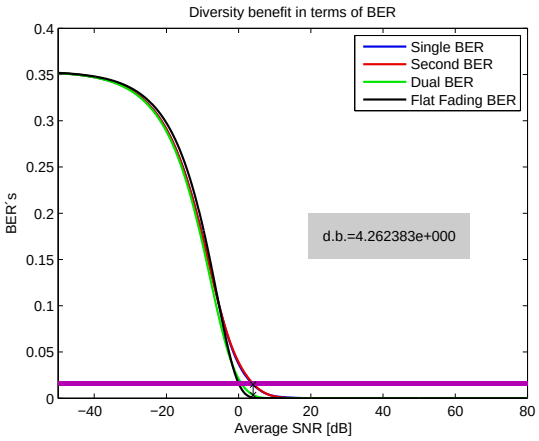

Figure 4.12: Normalized BER curves for the scenario 1 test 1, Stand/Sit/Stand

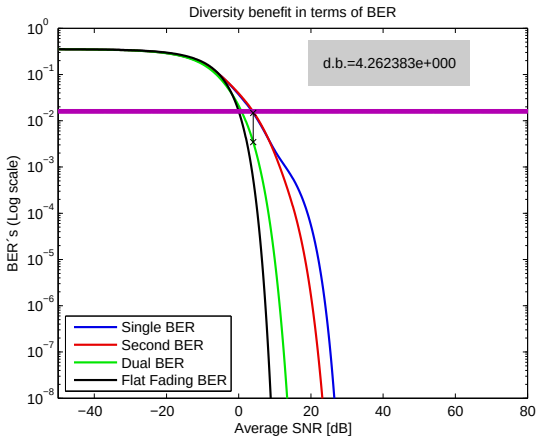

Figure 4.13: Normalized BER curves for the scenario 1 test 1, Stand/Sit/Stand in log scale

three kind of movements the BER curves were defined for the same SNR_{Tx}.

All the BER figures are attached in the Annex, so in this section there will be only some of them to illustrate some cases. Besides, they will be zoomed in the region where the considered SNR_{Tx} is located.

Regarding the *Laying on a bed* case, in scenarios 1 and 5 the single-link appears to have better BER performance than the dual-link, but the difference is so inappreciable that all the channels seem to have the same curves, as it can be seen in figure 4.14. Scenario 4 is an example where a BER benefit can't be achieved, since channel 2 is worse in terms of averaged power and variance. So, as figure 4.15 depicts, the single transmission is better than the dual-link, since the added one doesn't contribute with any improvement.

In figures 4.16 and 4.17 are represented two other cases from scenarios 2 and 3, where the added channel has better curves than the single one, so a BER benefit can be achieved. Both tests have the single link with less averaged power than the added one but with the variance of the added link worse than the single one.

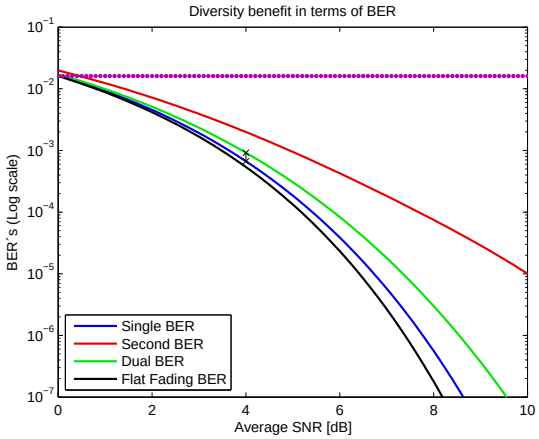

Figure 4.14: Normalized BER curves for the scenario 1 test 1, Laying

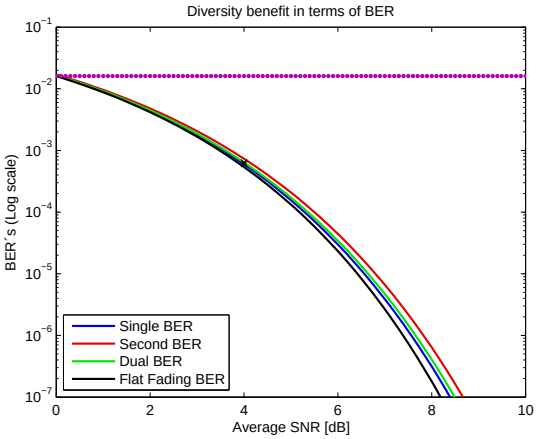

Figure 4.15: Normalized BER curves for the scenario 4 test 1, Laying

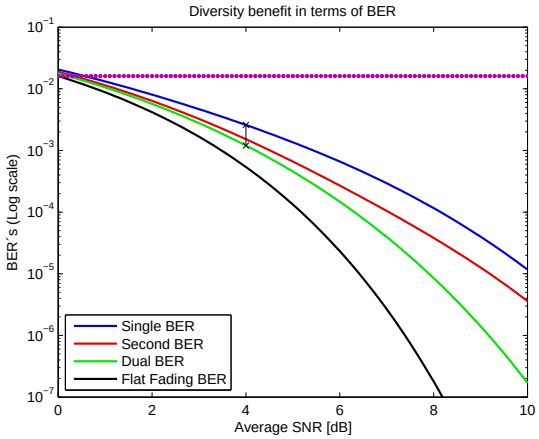

Figure 4.16: Normalized BER curves for the scenario 2 test 2, Laying

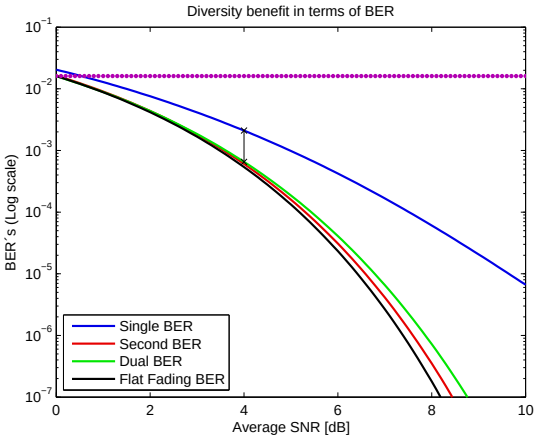

Figure 4.17: Normalized BER curves for the scenario 3 test 1, Laying

In the *Stand-up/Sit-down/Stand-up* case, scenario 2 has the same characteristics than in the *Walking* one, so it is commented then. In scenarios 4 and 5, channel 2 is much more worse in terms of averaged power, but much better in terms of variance. So, the overall results in a BER benefit. In scenarios 1 and 3 in some tests a benefit is achieved, but in others the single transmission reaches better BER results, although dual-link is very close to it. Two examples of these cases are displayed in figures 4.18 and 4.19.

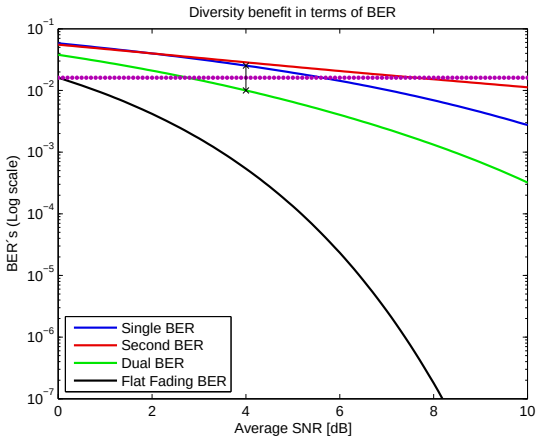

Figure 4.18: Normalized BER curves for the scenario 5 test 2, Stand/Sit/Stand

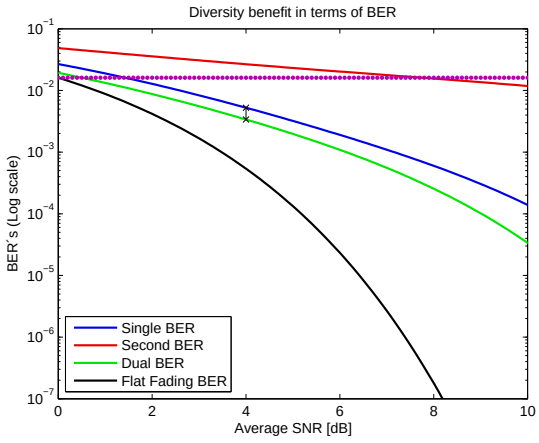

Figure 4.19: Normalized BER curves for the scenario 3 test 2, Stand/Sit/Stand

In the curves related to the *Walking* movement, in scenarios 2 and 3 it is where a higher benefit is achieved. As an example, in scenario 3, test 1 has channel 1 with worse power in average than channel 2, but channel 2 has a higher variance, so the added channel contributes to improve the channel power but it doesn't with the variance. Unlike in test 2, where channel 2 is worse in terms of averaged power, but it contributes positively to the variance. Therefore, in both cases there is an improvement of the dual-link BER regarding the single one, as depicted in figures 4.20 and 4.21.

In scenarios 1, 4 and 5 the BER curves of single and dual transmissions are very close, so a lower benefit can be reached. It is understandable from scenarios 4, where the channels are very similar, or 5, where the channels are overlapped. The problem with scenario 1 may be that the single transmission is the one from the shoulder to the hip, that in the case of walking has less fades than channel 2, which has the source in an arm that swings. So, channels should have been exchanged. Figures 4.22 and 4.23 show two of these measurements.

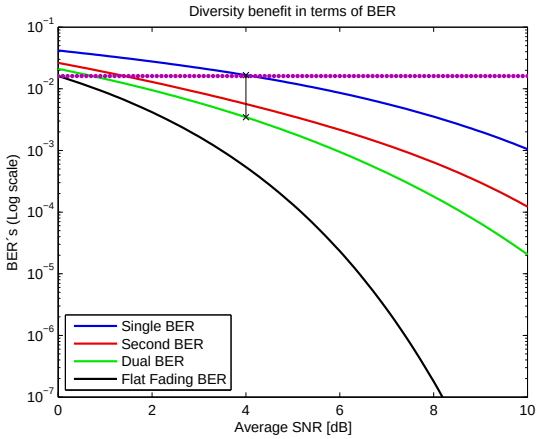

Figure 4.20: Normalized BER curves for the scenario 3 test 1, Walking

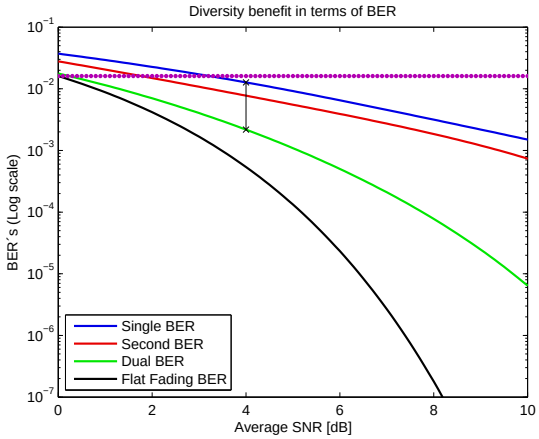

Figure 4.21: Normalized BER curves for the scenario 3 test 2, Walking

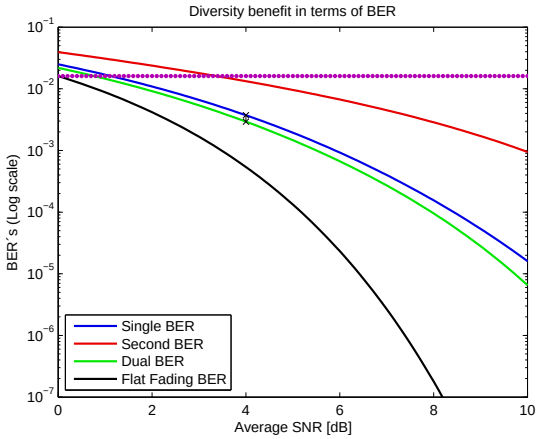

Figure 4.22: Normalized BER curves for the scenario 5 test 2, Walking

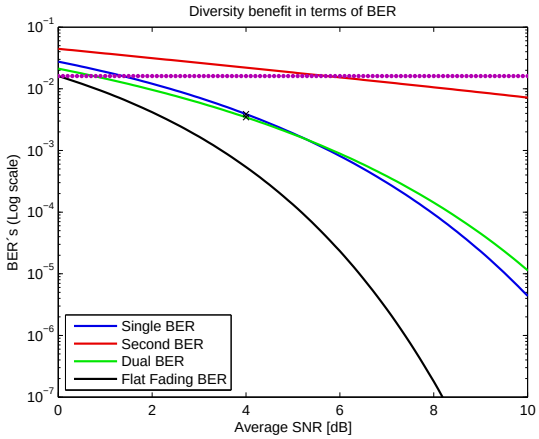

Figure 4.23: Normalized BER curves for the scenario 1 test 2, Walking

In the following figures (4.24, 4.25, 4.26), the values of the BER normalized benefit at 4 dB of output averaged SNR are shown according to each movement and all its scenarios. If the BER benefit is 1 it means that single and dual link has the same BER output for that SNR, so no improvement has been achieved, as well as if BER benefit is lower than 1, which means that the single link has a better BER performance than the dual one. In these results, it can be seen that it is more feasible to benefit from the diversity scheme in those cases where the person moves.

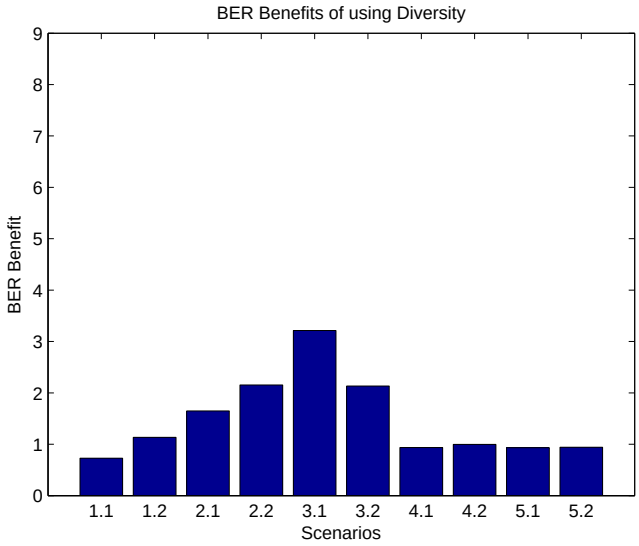

Figure 4.24: BER benefit of using diversity, Laying

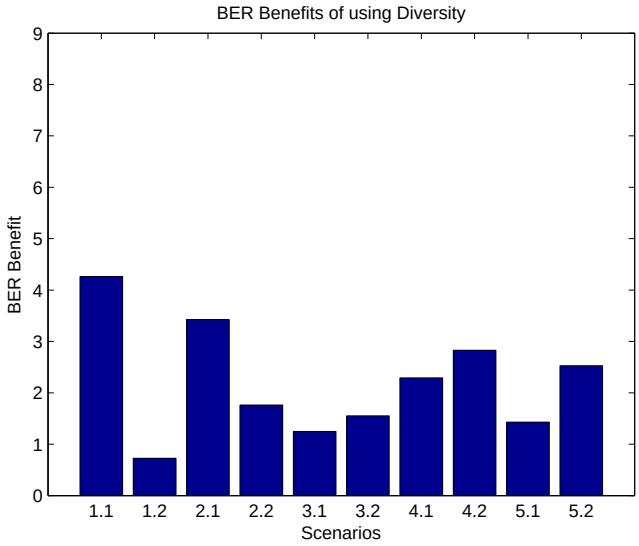

Figure 4.25: BER benefit of using diversity, Stand/Sit/Stand

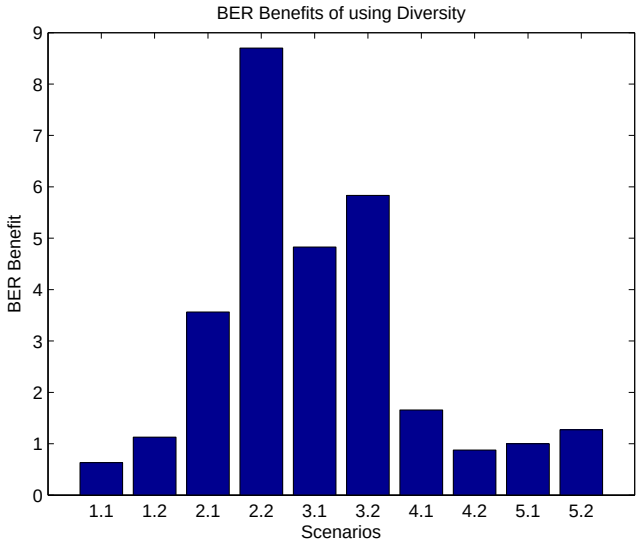

Figure 4.26: BER benefit of using diversity, Walking

These BER benefits can be matched with the correlation coefficients to see how this two magnitudes are related (see figures 4.27, 4.28, 4.29).

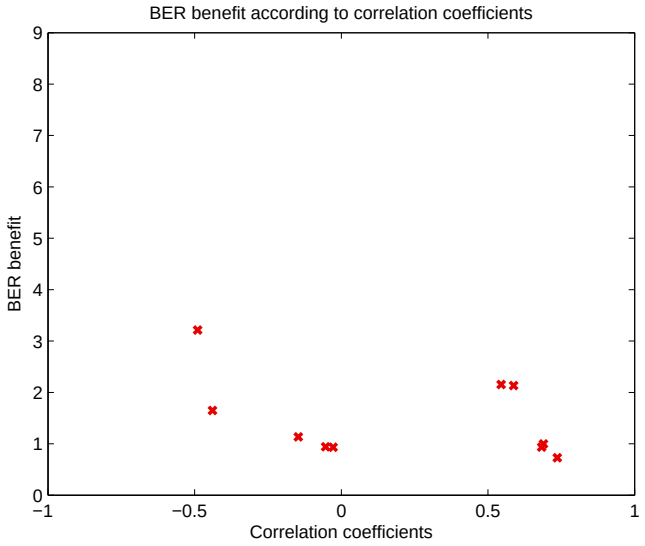

Figure 4.27: BER benefit according to correlation coefficients, Laying

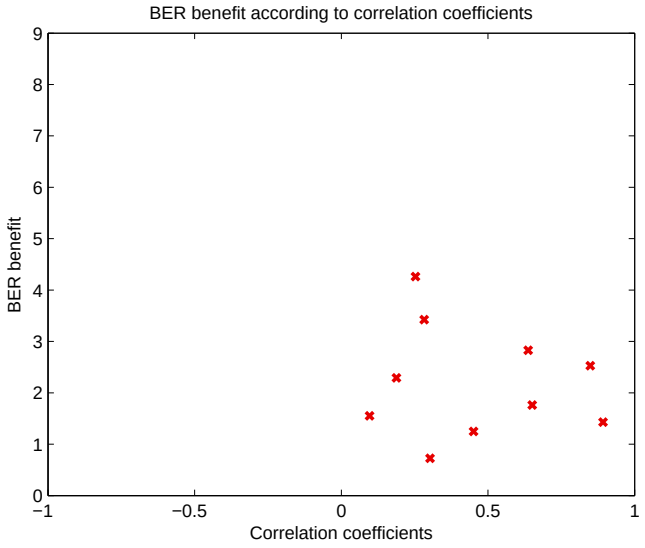

Figure 4.28: BER benefit according to correlation coefficients, Stand/Sit/Stand

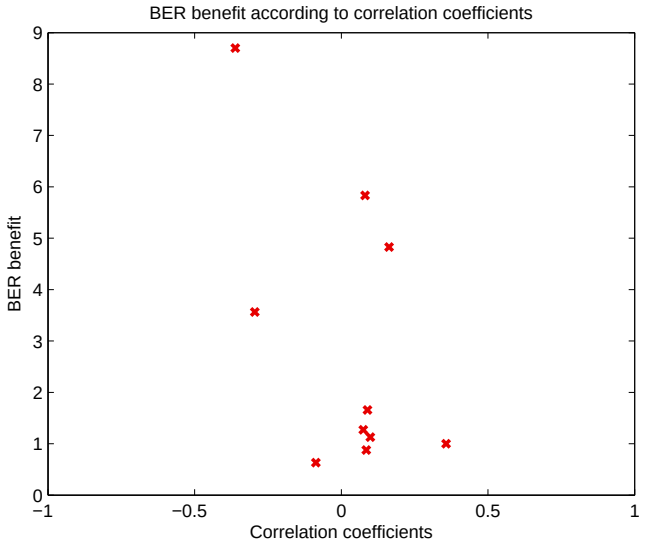

Figure 4.29: BER benefit according to correlation coefficients, Walking

4.3 Analysis on variance benefits of using diversity

Besides the improvement in the system's BER performance, the use of spatial diversity provides a variance reduction of the cooperative channel regarding the variance of the single link. This reduction depends largely on the correlation coefficients between the two cooperative channels. If both channels are correlated, the fading affects the two of them in the same way, so the variance of the dual link will be the same that if a single link was being used, or even higher if the channel added to cooperate with the single link has higher variance.

Nevertheless, if both channels are uncorrelated, the fading doesn't affect at the same time in each channel, so the combination of both channels will have less variance than the single link, as long as the added channel has better performance in terms of variance than the single channel. This variance benefit is analyzed by means of the S-parameters obtained with the VNA.

The parameter S_{21} characterizes the channel for the single link, so the SNR for the single transmission will be:

$$SNR_S = \frac{|h_1|^2}{\sigma_{n1}^2}$$

where $|h_1|^2 = |S_{21}|^2$ and σ_{n1}^2 is the noise in this channel.

When a dual transmission is being carried out, the joined channel can be seen as a combination of the two single channels with half of power each one, so the total power remains the same:

$$|h_D|^2 = \frac{|h_1|^2 + |h_2|^2}{2}$$

where similarly to the above, $|h_2|^2 = |S_{31}|^2$. So the SNR of the dual link will be:

$$SNR_D = \frac{|h_1|^2 + |h_2|^2}{2\ \sigma_N^2}$$

where $\sigma_N^2 = \sigma_{n1}^2 + \sigma_{n2}^2$. This equation is corresponded with eq. 4.1 used in the test bed, since in the test bed the diagonals of the channel gain matrix for the dual transmission had already half of the power of the single link.

If the channels are named as $x_1 = |h_1|^2$ and $x_2 = |h_2|^2$, their correlation coefficient in the dual transmission will be expressed as eq.4.4, the same used by Matlab (eq.3.1).

$$\rho_{\frac{x_1}{2},\frac{x_2}{2}} = \frac{E\{(\frac{x_1}{2} - E\{\frac{x_1}{2}\})(\frac{x_2}{2} - E\{\frac{x_2}{2}\})\}}{\sqrt{E\{((\frac{x_1}{2})^2 - E^2\{\frac{x_1}{2}\})E\{((\frac{x_2}{2})^2 - E^2\{\frac{x_2}{2}\})}}$$

$$\rho_{\frac{x_1}{2},\frac{x_2}{2}} = \frac{E\{\frac{x_1 \cdot x_2}{4}\} - E\{\frac{x_1}{2}\}E\{\frac{x_2}{2}\}}{\sigma_{\frac{x_1}{2}} \ \sigma_{\frac{x_2}{2}}} \tag{4.4}$$

The variance of the dual transmission channel is calculated as:

$$\sigma^2_{|h_D|^2} = \sigma^2(\frac{x_1 + x_2}{2}) = E\{(\frac{x_1 + x_2}{2} - E\{\frac{x_1 + x_2}{2})^2\} =$$

$$= E\{(\frac{x_1}{2})^2\} - E^2\{\frac{x_1}{2}\} + E\{(\frac{x_2}{2})^2\} - E^2\{\frac{x_2}{2}\} + 2E\{\frac{x_1 \cdot x_2}{4}\} - 2E\{\frac{x_1}{2}\}E\{\frac{x_2}{2}\}$$

Using eq. 4.4, the variance is finally obtained:

$$\sigma^2_{|h_D|^2} = \sigma^2_{\frac{x_1}{2}} + \sigma^2_{\frac{x_2}{2}} + 2 \ \rho_{\frac{x_1}{2},\frac{x_2}{2}} \ \sigma_{\frac{x_1}{2}} \ \sigma_{\frac{x_2}{2}} \tag{4.5}$$

To relate $\sigma^2_{\frac{x_1}{2}}$ and $\sigma^2_{\frac{x_2}{2}}$ from the dual case transmission, which have half of the power that a single link has, with the σ^2_{x1} of the single case transmission:

$$\sigma^2_{\frac{x_1}{2}} = E\{(\frac{x_1}{2} - E\{\frac{x_1}{2})^2\} = \frac{E\{x_1^2\}}{4} - \frac{E^2\{x_1\}}{4} = \frac{\sigma^2_{x1}}{4} \tag{4.6}$$

If the presumption $\sigma^2_{\frac{x_1}{2}} \approx \sigma^2_{\frac{x_2}{2}}$ is accepted to illustrate a simple case, then the bounds of $\sigma^2_{|h_D|^2}$ depending on the correlation coefficient are:

If $\rho_{\frac{x_1}{2},\frac{x_2}{2}} = 1$ (the channels are correlated)

then $\sigma^2_{|h_D|^2} = \frac{\sigma^2_{x1}}{4} + \frac{\sigma^2_{x1}}{4} + 2 \ \frac{\sigma_{x1}}{2} \ \frac{\sigma_{x1}}{2} \approx \sigma^2_{x1}$

If $\rho_{\frac{x_1}{2},\frac{x_2}{2}} = 0$ (the channels are uncorrelated)

then $\sigma^2_{|h_D|^2} = \frac{\sigma^2_{x1}}{4} + \frac{\sigma^2_{x1}}{4} \approx \frac{\sigma^2_{x1}}{2}$

If $\rho_{\frac{x_1}{2},\frac{x_2}{2}} = -1$ (the channels are anticorrelated)

then $\sigma^2_{|h_D|^2} \approx 0$

To sum up,

$$\sigma^2_{|h_D|^2} \approx \begin{cases} \sigma^2_{x1} & \text{if } \rho_{\frac{x_1}{2},\frac{x_2}{2}} = 1 \\ \frac{\sigma^2_{x1}}{2} & \text{if } \rho_{\frac{x_1}{2},\frac{x_2}{2}} = 0 \\ 0 & \text{if } \rho_{\frac{x_1}{2},\frac{x_2}{2}} = -1 \end{cases}$$

In order to obtain the benefits of transmitting through two channels instead of one, the variance of $|S_{21}|^2$ parameter for the single link case must be calculated, as well as the variance of the $|S_D|^2$ parameter for the dual link case. Then, the fraction between them shows the diversity benefit in terms of variance.

$$Variance\ \ benefit \ = \ \frac{\sigma^2_S}{\sigma^2_D} \tag{4.7}$$

It can be seen that in the case of $\rho_{\frac{x_1}{2},\frac{x_2}{2}} = -1$ the variance benefit tends to infinite since the dual channel tends to a flat channel, but this is only assuming that both variances are similar.

However, $\sigma^2_{\frac{x_1}{2}} \approx \sigma^2_{\frac{x_2}{2}}$ does not occur in the measurements done. Actually, $\sigma^2_{\frac{x_1}{2}} >> \sigma^2_{\frac{x_2}{2}}$ in many cases. Therefore, the bounds of $\sigma^2_{|h_D|^2}$ are different from the above and so do the values of the benefit. Similarly to the relationship $\sigma^2_{\frac{x_1}{2}} = \frac{\sigma^2_{x1}}{4}$ that is still valid, $\sigma^2_{\frac{x_2}{2}} = \frac{\sigma^2_{x2}}{4}$. By them, the bounds of the variance of the dual case can be re-calculated :

If $\rho_{\frac{x_1}{2},\frac{x_2}{2}} = 1$ (the channels are correlated)

then $\sigma^2_{|h_D|^2} = \frac{\sigma^2_{x1}}{4} + \frac{\sigma^2_{x2}}{4} + 2\ \frac{\sigma_{x1}}{2}\ \frac{\sigma_{x2}}{2} = \frac{\sigma^2_{x1}+\sigma^2_{x2}+2\sigma_{x1}\sigma_{x2}}{4}$

If $\rho_{\frac{x_1}{2},\frac{x_2}{2}} = 0$ (the channels are uncorrelated)

then $\sigma^2_{|h_D|^2} = \frac{\sigma^2_{x1}}{4} + \frac{\sigma^2_{x2}}{4} = \frac{\sigma^2_{x1}+\sigma^2_{x2}}{4}$

If $\rho_{\frac{x_1}{2},\frac{x_2}{2}} = -1$ (the channels are anticorrelated)

then $\sigma^2_{|h_D|^2} = \frac{\sigma^2_{x1}}{4} + \frac{\sigma^2_{x2}}{4} - 2\ \frac{\sigma_{x1}}{2}\ \frac{\sigma_{x2}}{2} = \frac{\sigma^2_{x1}+\sigma^2_{x2}-2\sigma_{x1}\sigma_{x2}}{4}$

So, the bounds of variance benefit are:

$$\begin{cases} Benefit_{min} = \frac{4\sigma^2_{x1}}{\sigma^2_{x1}+\sigma^2_{x2}+2\sigma_{x1}\sigma_{x2}} & \text{if } \rho_{\frac{x_1}{2},\frac{x_2}{2}} > 0 \\ Benefit_{max} = \frac{4\sigma^2_{x1}}{\sigma^2_{x1}+\sigma^2_{x2}} & \text{if } \rho_{\frac{x_1}{2},\frac{x_2}{2}} = 0 \\ Benefit_{max} = \frac{4\sigma^2_{x1}}{\sigma^2_{x1}+\sigma^2_{x2}-2\sigma_{x1}\sigma_{x2}} & \text{if } \rho_{\frac{x_1}{2},\frac{x_2}{2}} < 0 \end{cases}$$

In the following figures, besides of calculating the diversity benefit in terms of variance, represented by the red circles in the figures, its bounds are also shown. The continuous line represents the possible range of diversity values regarding ρ from $\rho = 1$ in the bottom to $\rho = 0$ in the upper side; while the dotted one represents the range of the anticorrelated cases until $\rho = -1$.

The first figure, 4.30, refers to the *Laying on a bed* case. As the rest of the figures it is zoomed to appreciate the values of the variance benefit, so the whole range for the anticorrelated cases can not be completed shown, but it is displayed in the figures attached in the Annex. In this case, benefit is achieved in scenario 5 and the tests with uncorrelated channels from scenarios 1 and 2.

In the first scenario, although the variance of the single link is worse than the added one, in one of the tests, the channels are correlated, so the benefit decreases; in the second scenario, there is a test where the channels are not correlated and benefits of using diversity could be achieved, but the variance of the added channel is higher than the one from the single.

In scenarios 3 and 4 the variance of the added channel is much higher than that one from the single one, so the fact of using a worse channel to improve the first one does not involve any variance reduction.

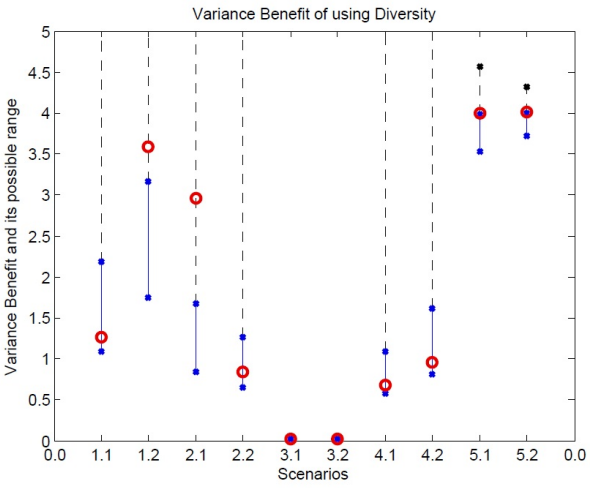

Figure 4.30: Variance benefit of using diversity, Laying

In the *Stand-up/Sit-down/Stand-up* case, more benefit of using diversity can be observed (figure 4.31). In almost all scenarios there is a reduction of the variance of the cooperative channel, specially in scenario 1, 4 and 5. In

scenario 2 there is a test where no benefit is achieved. This is again caused by the fact that the second link is worse in terms of variance. In scenario 1, any range can be seen since the variance of the single channel is much higher than the second channel.

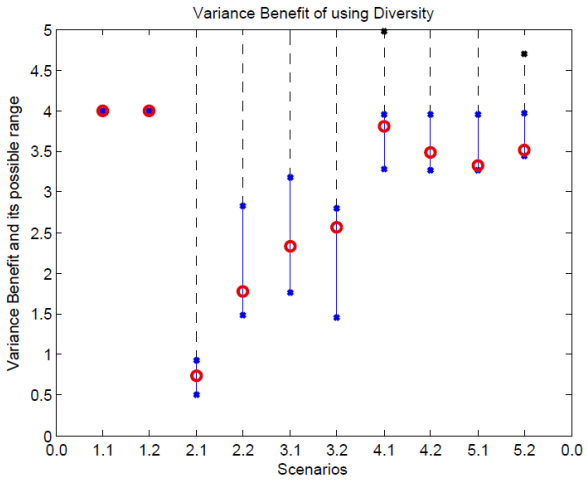

Figure 4.31: Variance benefit of using diversity, Stand/Sit/Stand

The case of the *Walking* movement is similar to the previous one. In general there is benefit of using two links instead of one, except for some particular cases: as figure 4.32 shows, in test 1 in scenarios 2 and 3 the variance of the second channel reduces the possibility of improving the system performance.

So, in general, in the dynamic measurements such as *Walking* and *Stand-up/Sit-down/Stand-up*, there are more chances to exploit spatial diversity and acquire more benefits in terms of variance. A parameter to have into account is the variance of the added channel, since it can change dramatically the variance benefit.

It also can be observed that a higher reduction of the cooperative link's variance can be achieved if both channels are anticorrelated. The relation between the correlation coefficients and the improvement in the variance of the dual link can be seen in figures 4.33, 4.34, 4.35.

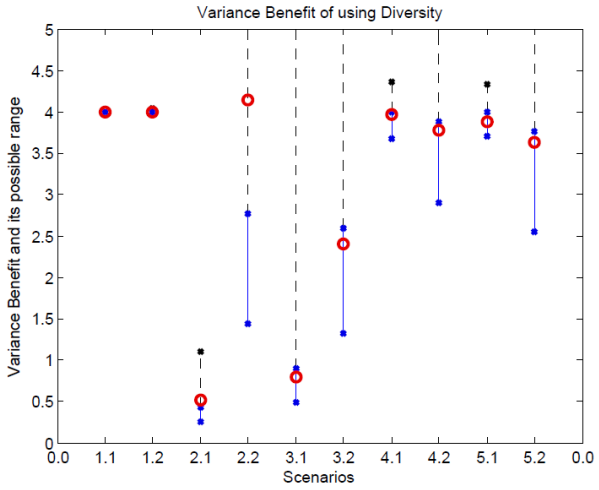

Figure 4.32: Variance benefit of using diversity, Walking

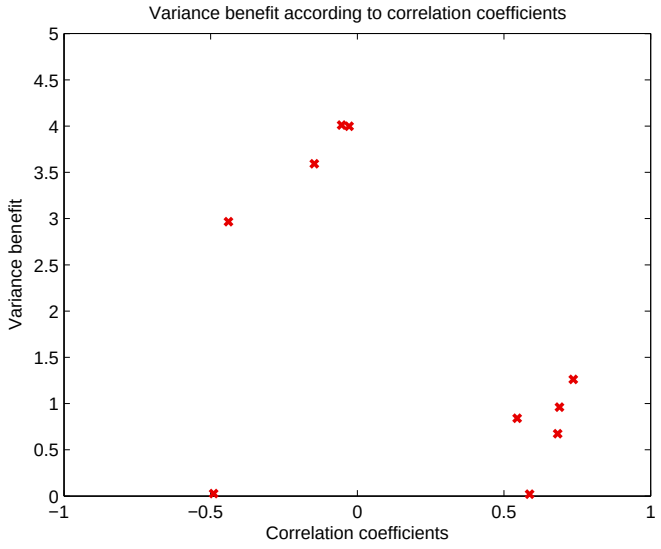

Figure 4.33: Variance benefit according to correlation coefficients, Laying

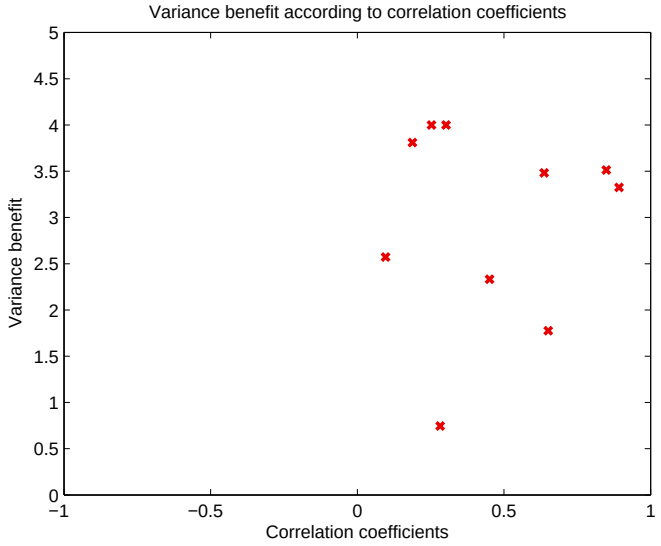

Figure 4.34: Variance benefit according to correlation coefficients, Stand/Sit/Stand

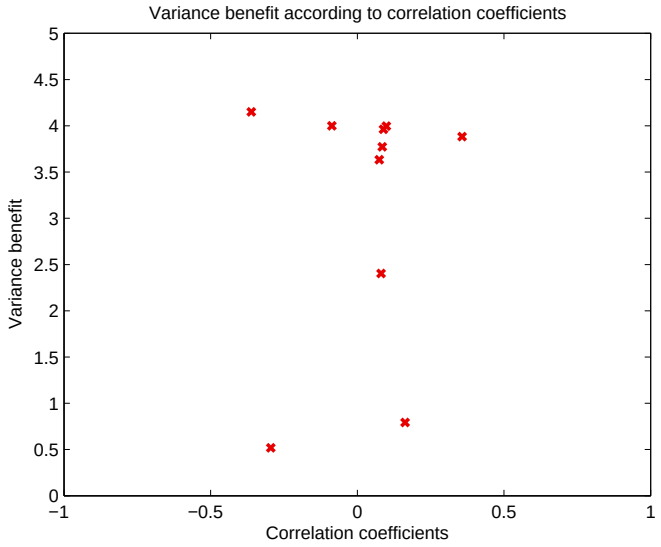

Figure 4.35: Variance benefit according to correlation coefficients, Walking

In the following figures: 4.36, 4.37 and 4.38 both benefits are plotted altogether to see how they are related.

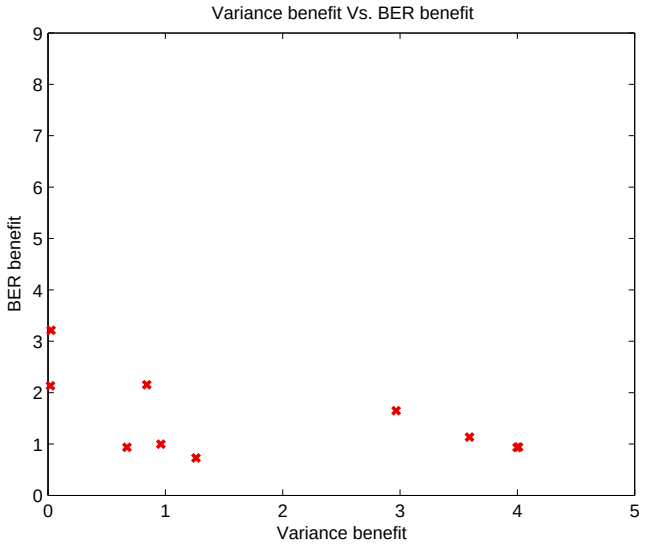

Figure 4.36: BER benefit according to variance benefit, Laying

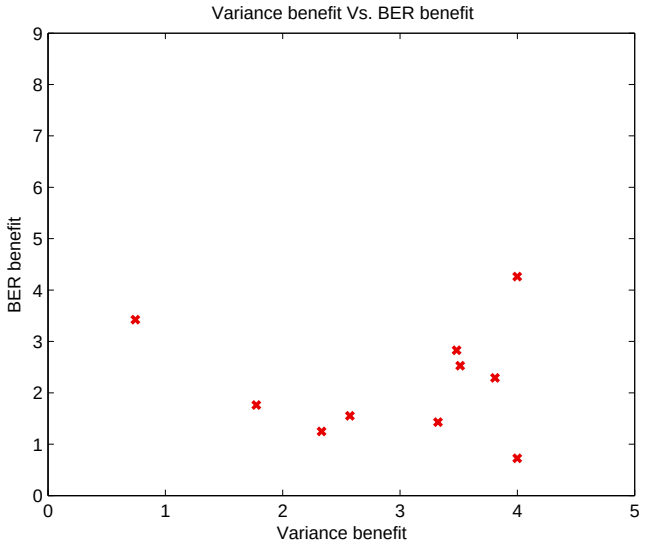

Figure 4.37: BER benefit according to variance benefit, Stand/Sit/Stand

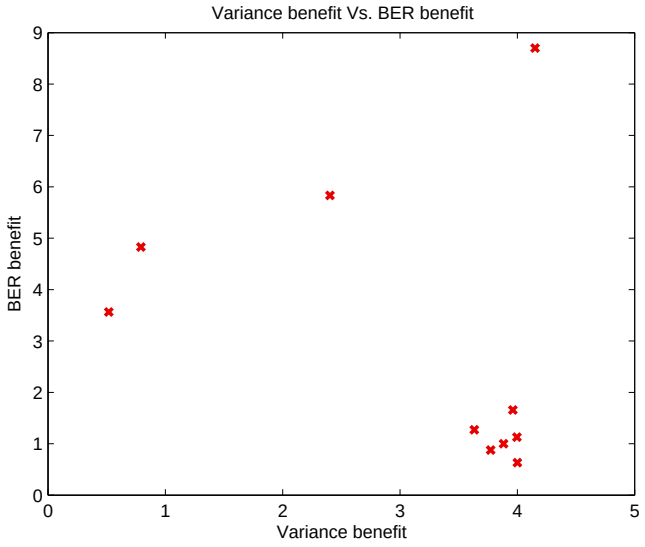

Figure 4.38: BER benefit according to variance benefit, Walking

Chapter 5

Conclusions and Future work

This last chapter contains the final thoughts of this project. After all the measurements and their analysis, some of the objectives have been achieved while other have to be further developed to their fully accomplishment. As an overview, it could be said that the main goals are reached or approached.

If the objectives set at the beginning of the document are recovered, it could be evaluated their degree of accomplishment:

- **Investigate the BER performance for both the single and the dual-link and the channel diversity gain for each measurement.**

  As explained before, the test bed couldn't provide consistent BER results, so the BER performance obtained by this project is an equivalent not the real one. Nevertheless, it has been possible to present a comparison between both dual and single transmissions and their BERs results.

  It can be observed that in the dynamic movements the diversity gain is more achieved than in the *Laying on a bed* case. It's understandable since in the static case less antennas suffer from deep fades because there is no body movement which can affect momentarily the transmission except from the breathing.

- **Analyze channel statistics.**

  A complete analysis of the channel have been carried out. In Chapter 3 the main statistics are presented in detail for each one of the measured movements and scenarios. An approach of the fading power distribution is also shown for each channel.

- Study the benefits of using diversity in terms of variance.

The reduction of the variance of the dual-link is also more feasible in *Stand-up/Sit-down/Stand-up* and *Walking* cases. In general, while the variance of the single link is higher than the channel added to cooperate, a significant reduction of the variance of the dual-link is achieved. It can be observed that if both channels are anticorrelated the benefit is even higher.

- Compare results from the VNA measurements and the test bed's, such as channel statistics of different movements of the body with the BER performance.

This particular objective was not possible to fully accomplish it since the BER results from the test bed were not consistent, so the results from independent devices couldn't be compared. Instead of them, the BERs were calculated from the VNA results to procure an idea of how they are related to the body movements.

In the dynamic cases, where the body movements cause deeper fades, there was a clearly advantage of using a cooperation link which leads to a combination of two channels to achieve a better BER performance. In the static case this BER improvement is not as noticeable as it is in the other two cases but it also exists.

- Trace a relation between diversity benefits and correlation coefficients between channels. As it can be seen in the figures where correlation coeffcients are plotted according to the BER and variance benefits, no clear relation can be traced. May be to determine the relation between correlation coefficients and BER, a normalization on the channel variance should be done, instead of analyze these benefits with two channels with very different variances. Therefore, a further study should be done regarding the correlations coefficients and diversity benefits to find a relation between them. There is no clear relation neither between both BER and variance benefits. So, this relation should be retained for future work.

As demonstrated, the skycross antennas are nos suitable to USRP kit due to different radiation pattern and the fast phase change they introduce. This leads to a bad estimation, so as future work this mismatch should be resolved. Different antennas should be used for this experiment or a new test bed developed. Therefore, the simultaneous measurements could be done, so some of the goals that weren't fully accomplished could be better analyzed.

Bibliography

[1] C.Oestges, B.Clerckx *"MIMO Wireless Communications"* Elsevier Science, May 2007.

[2] L. Liu, F. Keshmiri, S. van Roy, C. Craeye, P. De Doncker, C. Oestges *"Channel characterization and modelling in WBANs"* Wireless Acquisition and LInk for Body Information (WALIBI) Project, Région wallonne, Délivrable D3 Antennes et propagation pour réseaux de capteurs corporels, 2008-2009.

[3] J.G. Proakis *"Digital communications"* 4th ed., McGraw-Hill, NewYork, NY, 2001.

[4] H. H. Sneessens *"Coded transmission systems for the orthogonal relay channel"* Ph.D. dissertation, UCL, 2009.

[5] E. Jovanov, J. Price, D. Raskovic, K. Kavi, T. Martin, and R. Adhami *"Wireless personal area networks in telemedical environment"* Proc.3rd IEEE EMBS Inf. Technol. Appl. Biomed.-Workshop Int. Telemed. Inf. Soc. (ITAB ITIS 2000), Arlington, VA, Nov. 2000, pp. 22-27.

[6] T. G. Zimmerman *"Personal Area Networks: Near-field intrabody communication"* IBM Syst. J., vol. 35, no. 3-4, pp. 609-617, 1996.

[7] B. Heile, I. Gifford, and T. Siep *"The IEEE P802.15 working group for wireless personal area networks"* IEEE Netw., vol. 13, no. 4, pp. 4-5, Jul. 1999.

[8] K. van Dam, S. Pitchers, andM. Barnard *"From PAN to BAN: Why body area networks"* presented at the Wireless World Res. Forum 2, Helsinki, Finland, May 10-11, 2001.

[9] R. Schmidt, T. Norgall, J. Mörsdorf, J. Bernhard, and T. von der Grün *"Body area network BAN - a key infrastructure element for patient-centered medical applications"* Biomed. Tech. (Berl.), vol. 47, pp. 365-368, 2002.

[10] A. van Halteren, R. Bults, K.Wac, N. Dokovsky, G. Koprinkov, I.Widya, D. Konstantas, V. Jones, and R. Herzog *"Wireless body area networks for healthcare: The MobiHealth project"* inWearable eHealth Systems for Personalised Health Management: State of the Art and Future Challenges, vol. 108, Amsterdam, The Netherlands: IOS Press, 2004.

[11] R. S. H. Istepanian, E. Jovanov, and Y. T. Zhang *"Guest editorial introduction to the special section on M-health: Beyond seamless mobility and global wireless health-care connectivity"* IEEE Trans. Inf. Technol. Biomed., vol. 8, no. 4, pp. 405-414, Dec. 2004.

[12] K.Y. Yazdandoost and K. Sayrafian-Pour *"Channel Model for Body Area Network (BAN)"* IEEE P802.15 Working Group for Wireless Personal Area Networks (WPANs)

[13] Arie Reichman *"Standardization of Body Area Networks"* Ruppin Academic Center, November 2009.

[14] *"Statistical Characterization of 4 GHz Narrowband On-Body Propagation Channel"* COST 2100 TD (10)10031, Athens, Greece, February 2010.

[15] R. D'Errico and L. Ouvry *"Time-variant BAN channel channel characterization"* COST 2100 TD(09) 879, Valencia, Spain, May 2009.

[16] W. Scanlon and S. Cotton *"Understanding on-body fading channels at 2.45 GHz using measurements based on user state and environment"*. Antennas and Propagation Conference, 2008. LAPC 2008. Loughborough, 2008, pp.10-13.

[17] S. Cotton, G. Conway and W. Scanlon *"A Time-Domain Approach to the Analysis and Modeling of On-Body Propagation Characteristics Using Synchronized Measurements at 2.45 GHz"* Antennas and Propagation, IEEE Transactions on Volume:57, Issue:4, Part 1, pages:943-955, April 2009.

[18] Z. Hu, Y. Nechayev, P. Hall, C. Constantinou and Y. Hao *"Measurements and Statistical Analysis of On-Body. Channel Fading at 2.45 GHz"* IEEE Antennas Wireless Propag. Lett., vol. 6, pp. 612-615, 2007.

[19] S. L. Cotton and W. G. Scanlon *"An experimental investigation into the influence of user state and environment on fading characteristics in wireless body area networks at 2.45 GHz"* IEEE Trans. Wireless Commun., vol.8, no.1, pp. 6-12, Jan. 2009.

[20] M. Gallo, P. Hall, Y. Nechayev and M. Bozzetti *"Use of Animation Software in Simulation of On-Body Communications Channels at 2.45 GHz"* IEEE Antennas Wireless Propag. Lett., vol. 7, pp. 321-324, 2008.

[21] Raffaele DErrico, R. Rosini and M. Maman *"A Performance Evaluation of Cooperative Mechanisms in On-Body Area Networks"* COST 2100 TD(10)11083, Aalborg, Demark, June 2010.

[22] Jean-Marie Gorce, Claire Goursaud, Christophe Savigny, Guillaume Villemaud, Raffaele d'Errico, Franois Dehmas, Mickael Maman, Laurent Ouvry, Benoit Miscopein, Jean Schwoerer *"Cooperation mechanisms in BANs"* COST 2100 TD(09) 862, Valencia, Spain, May 2009.

[23] V. Bhatnagar *"Rapport sur les techniques de robustification et de garantie dintégrité"*. Wireless Acquisition and LInk for Body Information (WALIBI) Project, Région wallonne, Convention n616 449, October 2009.

[24] F. A. Hamza. *"The USRP under 1.5x Magnifying Lens!"*. The GNU Radio Project, Tech. Rep., June 2008.

[25] Agilent Technologies *"Data Sheet and Technical Specifications "*. Agilent 2-Port and 4-Port PNA-X Network Analyzer, 08/06/2010.

[26] Xiong, Fuqin *"Digital Modulation Techniques"* Artech House, 2000.

[27] D.Tse and P. Viswanath *"Fundamentals of Wireless Comunications"* Cambridge University Press, 2005.

Chapter 6

Annexes

Channels statistics

Scenario 1

L	Measurement	Mean [dB]	Std. [dB]	Corr.coeff
Test 1	$\|S_{21}\|^2$	-70.467153648906233	-158.1187023920331	0.736082123457947
	$\|S_{31}\|^2$	-74.531949227431426	-158.9276616874034	
Test 2	$\|S_{21}\|^2$	-71.754140831413935	-161.2625968889749	-0.146450170265789
	$\|S_{31}\|^2$	-76.814241190808801	-167.0523118996522	

Table 6.1: Values for *Laying on a bed* in Scenario 1

S	Measurement	Mean [dB]	Std. [dB]	Corr.coeff
Test 1	$\|S_{21}\|^2$	-36.267937823782404	-75.0973817751776	0.252752400809003
	$\|S_{31}\|^2$	-71.415649080146508	-146.1564251703816	
Test 2	$\|S_{21}\|^2$	-35.540627005203007	-0.728985429358227	0.302712322770482
	$\|S_{31}\|^2$	-72.907488901464035	-143.8910647852558	

Table 6.2: Values for *Stand/Sit/Stand* in Scenario 1

W	Measurement	Mean [dB]	Std. [dB]	Corr.coeff
Test 1	$\|S_{21}\|^2$	-31.846000968015034	-70.8448504756427	-0.086592891614365
	$\|S_{31}\|^2$	-67.720273746105164	-135.1430367199477	
Test 2	$\|S_{21}\|^2$	-46.713324484432832	-95.1378163495853	0.098785715964128
	$\|S_{31}\|^2$	-72.489121898924154	-142.1523703903967	

Table 6.3: Values for *Walking* in Scenario 1

Scenario 2

L	Measurement	Mean [dB]	Std. [dB]	Corr.coeff
Test 1	$\|S_{21}\|^2$	-78.216208245314505	-169.4975607064036	-0.439086721275998
	$\|S_{31}\|^2$	-76.511461836120205	-168.0996973416310	
Test 2	$\|S_{21}\|^2$	-78.577194542120367	-166.9763592467351	0.544856995146602
	$\|S_{31}\|^2$	-76.528189325519250	-163.6457939202085	

Table 6.4: Values for *Laying on a bed* in Scenario 2

S	Measurement	Mean [dB]	Std. [dB]	Corr.coeff
Test 1	$\|S_{21}\|^2$	-64.129752000404295	-130.5013159933614	0.282457558273767
	$\|S_{31}\|^2$	-62.290478071540193	-125.2653630260332	
Test 2	$\|S_{21}\|^2$	-62.759892129324264	-122.4780915679497	0.650714937225285
	$\|S_{31}\|^2$	-65.566045692732729	-126.3031015336916	

Table 6.5: Values for *Stand/Sit/Stand* in Scenario 2

W	Measurement	Mean [dB]	Std. [dB]	Corr.coeff
Test 1	$\|S_{21}\|^2$	-68.106087677034722	-135.5931134335915	-0.294911089255988
	$\|S_{31}\|^2$	-65.477170055081700	-126.3325681445667	
Test 2	$\|S_{21}\|^2$	-67.810630320122755	-133.3424548602458	-0.361623099844525
	$\|S_{31}\|^2$	-68.966478798070071	-136.8382211883325	

Table 6.6: Values for *Walking* in Scenario 2

Scenario 3

L	Measurement	Mean [dB]	Std. [dB]	Corr.coeff
Test 1	$\|S_{21}\|^2$	-86.211036313751094	-181.0452906470297	-0.489802704457113
	$\|S_{31}\|^2$	-69.432088423993790	-158.8659396731587	
Test 2	$\|S_{21}\|^2$	-84.980506090377460	-176.4548832344004	0.587230548896784
	$\|S_{31}\|^2$	-68.795808337301082	-153.9679249523644	

Table 6.7: Values for *Laying on a bed* in Scenario 3

S	Measurement	Mean [dB]	Std. [dB]	Corr.coeff
Test 1	$\|S_{21}\|^2$	-64.627856650749777	-126.2637285982537	0.450720397474439
	$\|S_{31}\|^2$	-67.106181846897712	-132.1507698660959	
Test 2	$\|S_{21}\|^2$	-61.743873022466161	-127.3687559985855	0.096514766609187
	$\|S_{31}\|^2$	-65.720802409807945	-131.0511346408570	

Table 6.8: Values for *Stand/Sit/Stand* in Scenario 3

W	Measurement	Mean [dB]	Std. [dB]	Corr.coeff
Test 1	$\|S_{21}\|^2$	-63.105339321573283	-128.1559226462167	0.162816073253890
	$\|S_{31}\|^2$	-58.929621368707132	-122.7819606318004	
Test 2	$\|S_{21}\|^2$	-61.900646316537745	-125.5655895892926	0.081003352282105
	$\|S_{31}\|^2$	-61.655344300085915	-128.2041278061639	

Table 6.9: Values for *Walking* in Scenario 3

Scenario 4

L	Measurement	Mean [dB]	Std. [dB]	Corr.coeff
Test 1	$\|S_{21}\|^2$	-64.111147716157291	-148.5369667912083	0.682969670229604
	$\|S_{31}\|^2$	-65.094052278014388	-144.2290543385064	
Test 2	$\|S_{21}\|^2$	-63.764853930809338	-152.1605105236543	0.689030829671845
	$\|S_{31}\|^2$	-64.326924420408176	-167.0523118996522	

Table 6.10: Values for *Laying on a bed* in Scenario 4

S	Measurement	Mean [dB]	Std. [dB]	Corr.coeff
Test 1	$\|S_{21}\|^2$	-66.214604425714356	-132.3885050652826	0.188159078212253
	$\|S_{31}\|^2$	-75.268147449006904	-152.0853430255143	
Test 2	$\|S_{21}\|^2$	-68.120421732882306	-133.9641525264085	0.637185595277058
	$\|S_{31}\|^2$	-75.672652906337859	-153.3330484078232	

Table 6.11: Values for *Stand/Sit/Stand* in Scenario 4

W	Measurement	Mean [dB]	Std. [dB]	Corr.coeff
Test 1	$\|S_{21}\|^2$	-59.624257737437247	-121.9510099113886	0.089069551060213
	$\|S_{31}\|^2$	-74.894236160323317	-149.2961032073368	
Test 2	$\|S_{21}\|^2$	-66.880011927401313	-138.9666088651008	0.085270516818726
	$\|S_{31}\|^2$	-77.033146082239412	-154.1373537857428	

Table 6.12: Values for *Walking* in Scenario 4

Scenario 5

L	Measurement	Mean [dB]	Std. [dB]	Corr.coeff
Test 1	$\|S_{21}\|^2$	-67.465578246311168	-159.8052756349522	-0.027758100575641
	$\|S_{31}\|^2$	-85.117013859586876	-183.5868169185016	
Test 2	$\|S_{21}\|^2$	-66.906873348640772	-156.7252958594865	-0.053603043037532
	$\|S_{31}\|^2$	-87.018758821888525	-185.3078579068819	

Table 6.13: Values for *Laying on a bed* in Scenario 5

S	Measurement	Mean [dB]	Std. [dB]	Corr.coeff
Test 1	$\|S_{21}\|^2$	-58.916450629582322	-113.0489464799754	0.892359576452611
	$\|S_{31}\|^2$	-69.949713917979437	-132.4278673743293	
Test 2	$\|S_{21}\|^2$	-60.937883489165841	-115.3401443285699	0.849058234684852
	$\|S_{31}\|^2$	-72.036867359749607	-137.4946346648850	

Table 6.14: Values for *Stand/Sit/Stand* in Scenario 5

W	Measurement	Mean [dB]	Std. [dB]	Corr.coeff
Test 1	$\|S_{21}\|^2$	-56.226732100753765	-117.1552067122438	0.357067500426457
	$\|S_{31}\|^2$	-72.460584356432378	-145.1691044082677	
Test 2	$\|S_{21}\|^2$	-55.198345079400667	-114.6391656604478	0.075043696143138
	$\|S_{31}\|^2$	-64.918360602238948	-126.6318705977175	

Table 6.15: Values for *Walking* in Scenario 5

Benefits in terms of variance

In this section the figures with the whole range of variance benefit for the anticorrelated cases.

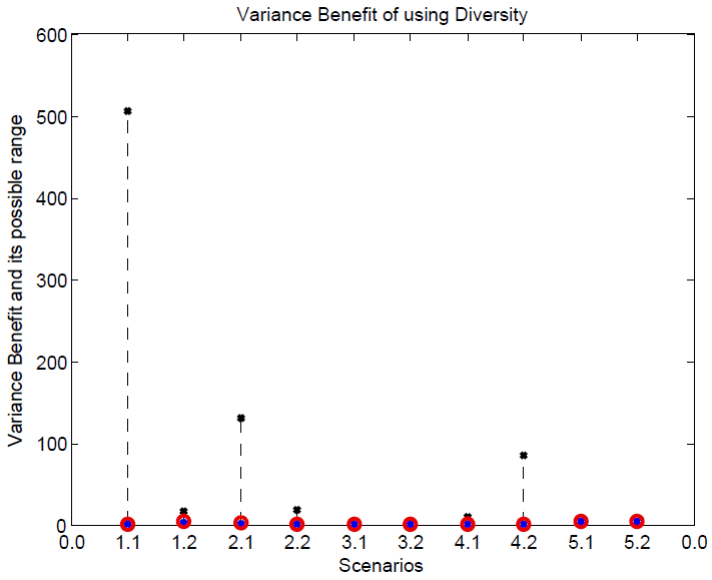

Figure 6.1: Variance benefit of using diversity, Laying

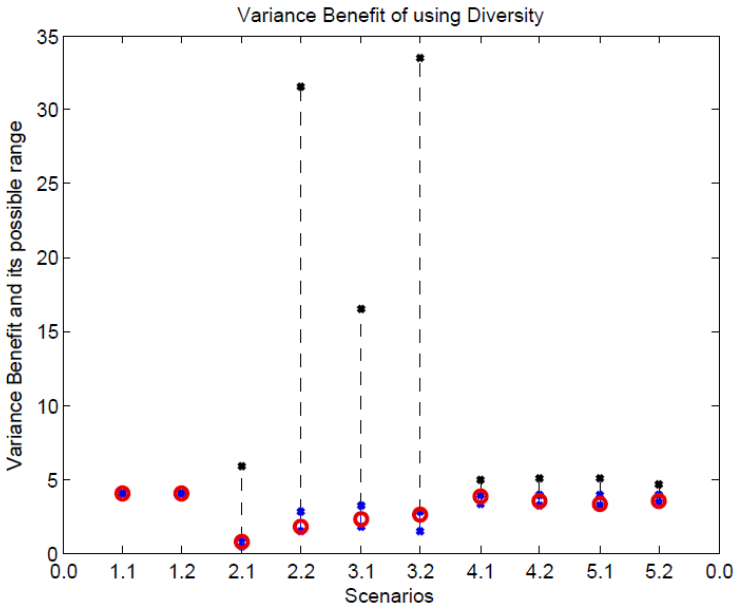

Figure 6.2: Variance benefit of using diversity, Stand/Sit/Stand

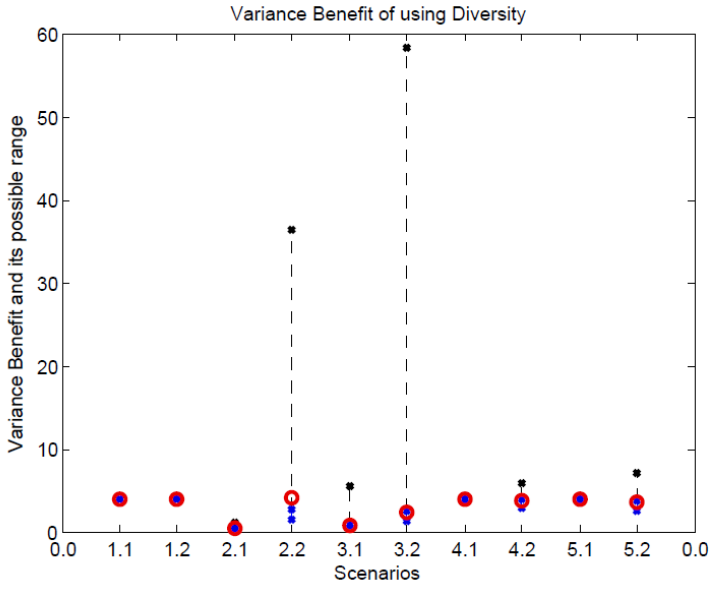

Figure 6.3: Variance benefit of using diversity, Walking

BER curves

Laying on a bed

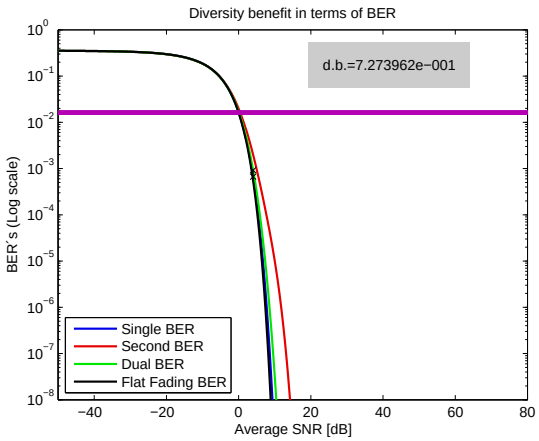

Figure 6.4: Normalized BER curves for the scenario 1 test 1, Laying

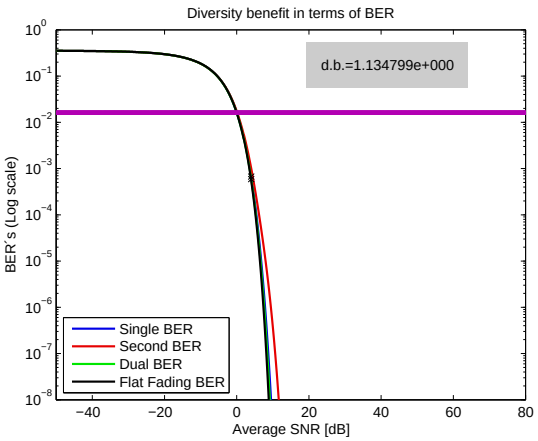

Figure 6.5: Normalized BER curves for the scenario 1 test 2, Laying

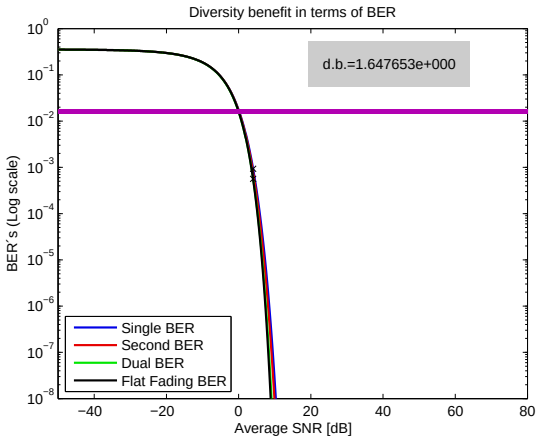

Figure 6.6: Normalized BER curves for the scenario 2 test 1, Laying

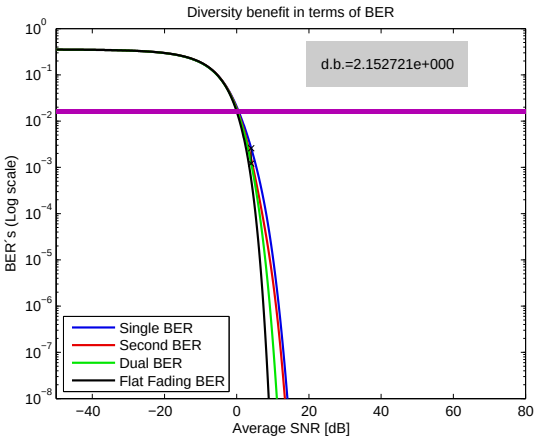

Figure 6.7: Normalized BER curves for the scenario 2 test 2, Laying

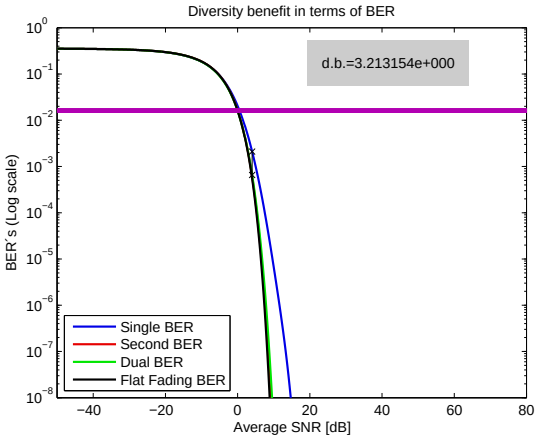

Figure 6.8: Normalized BER curves for the scenario 3 test 1, Laying

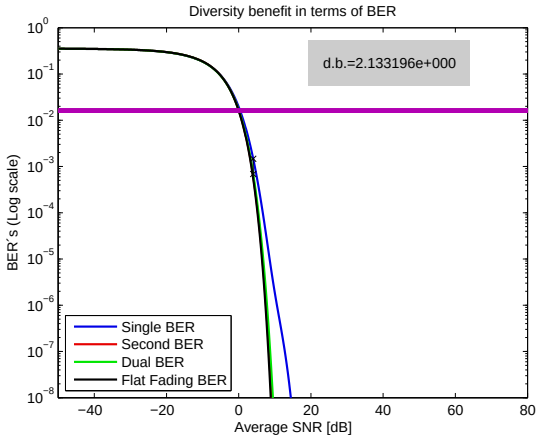

Figure 6.9: Normalized BER curves for the scenario 3 test 2, Laying

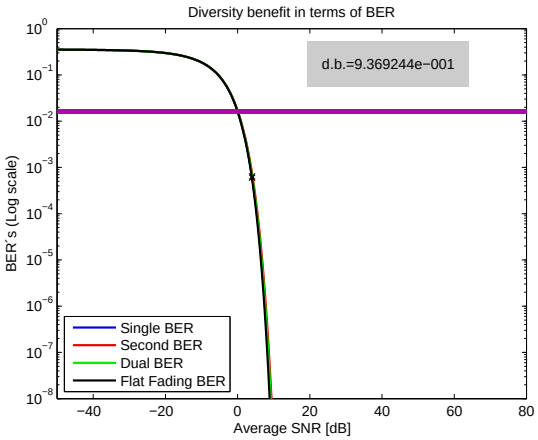

Figure 6.10: Normalized BER curves for the scenario 4 test 1, Laying

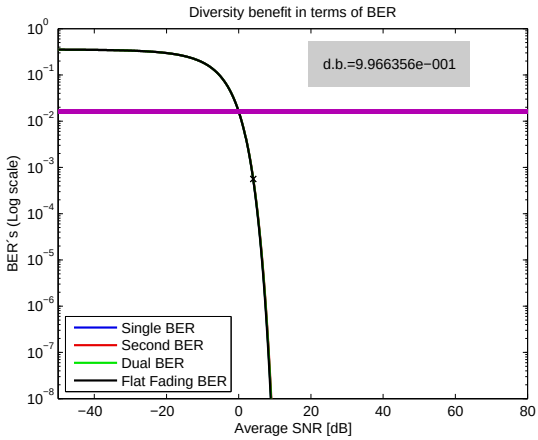

Figure 6.11: Normalized BER curves for the scenario 4 test 2, Laying

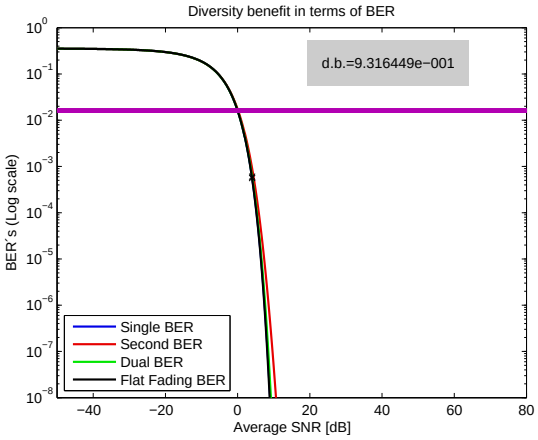

Figure 6.12: Normalized BER curves for the scenario 5 test 1, Laying

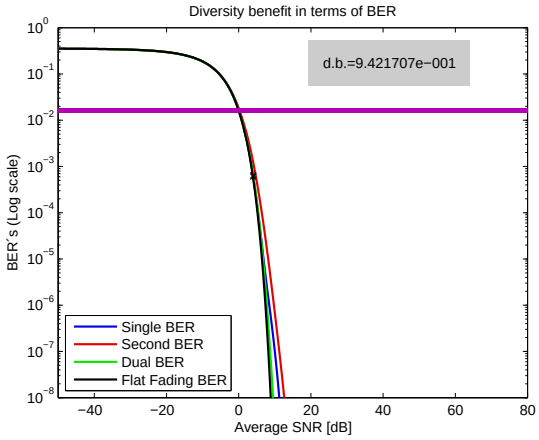

Figure 6.13: Normalized BER curves for the scenario 5 test 2, Laying

Stand-up/Sit-down/Stand

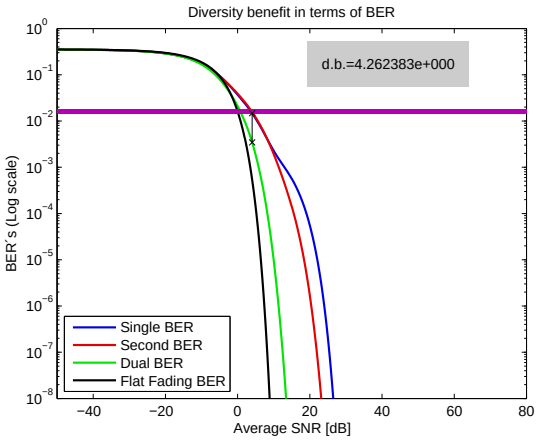

Figure 6.14: Normalized BER curves for the scenario 1 test 1,Stand/Sit/Stand

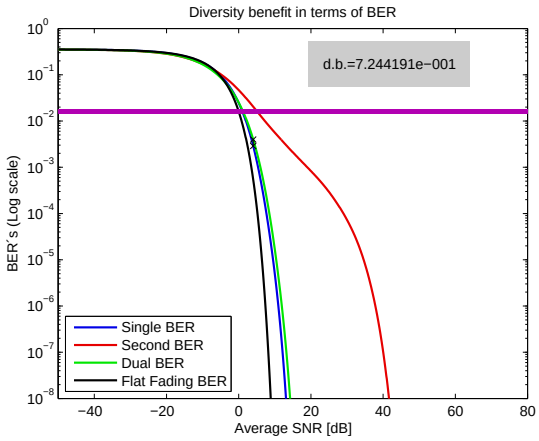

Figure 6.15: Normalized BER curves for the scenario 1 test 2, Stand/Sit/Stand

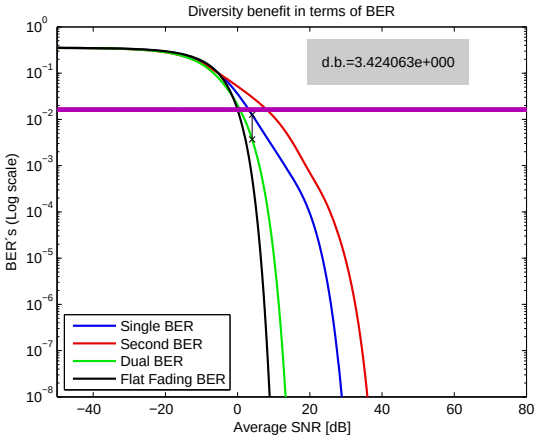

Figure 6.16: Normalized BER curves for the scenario 2 test 1, Stand/Sit/Stand

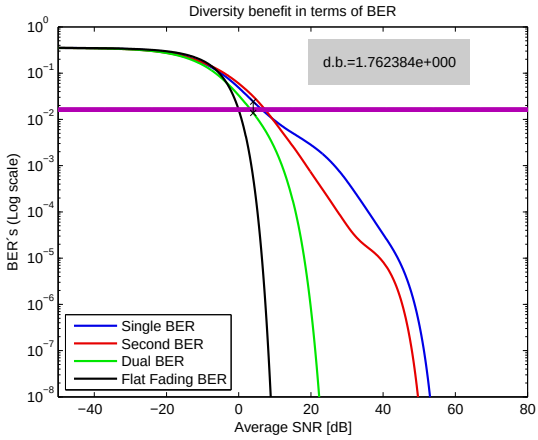

Figure 6.17: Normalized BER curves for the scenario 2 test 2, Stand/Sit/Stand

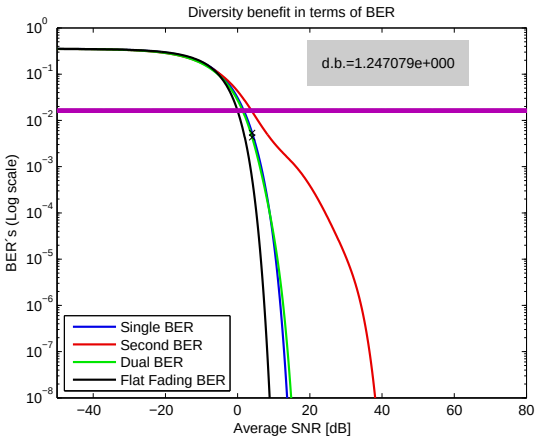

Figure 6.18: Normalized BER curves for the scenario 3 test 1, Stand/Sit/Stand

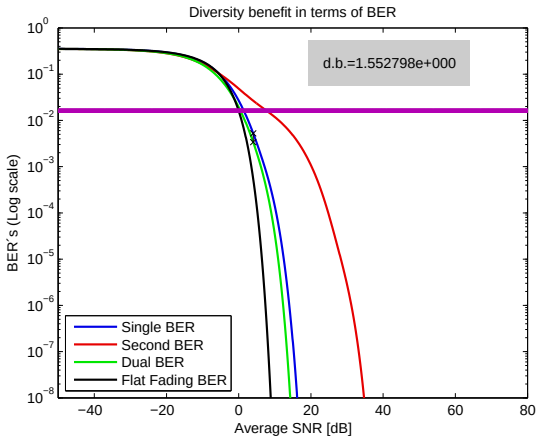

Figure 6.19: Normalized BER curves for the scenario 3 test 2, Stand/Sit/Stand

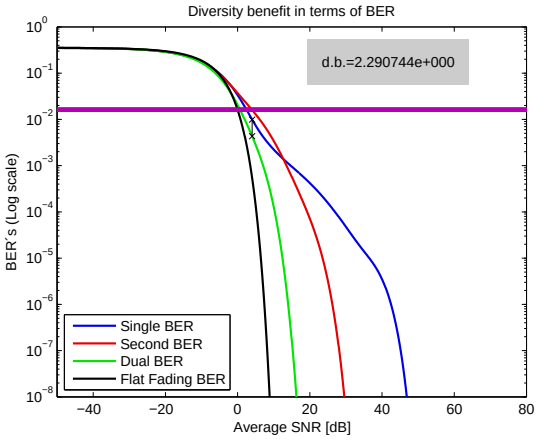

Figure 6.20: Normalized BER curves for the scenario 4 test 1, Stand/Sit/Stand

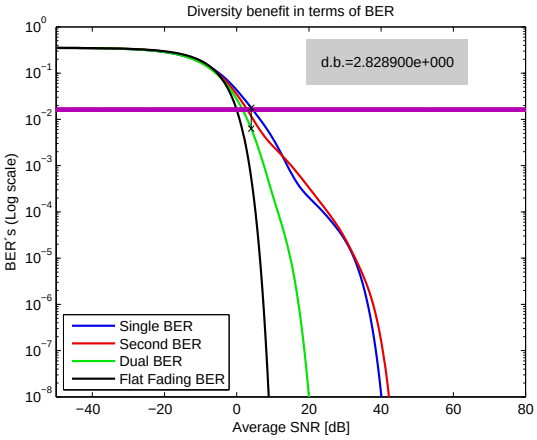

Figure 6.21: Normalized BER curves for the scenario 4 test 2, Stand/Sit/Stand

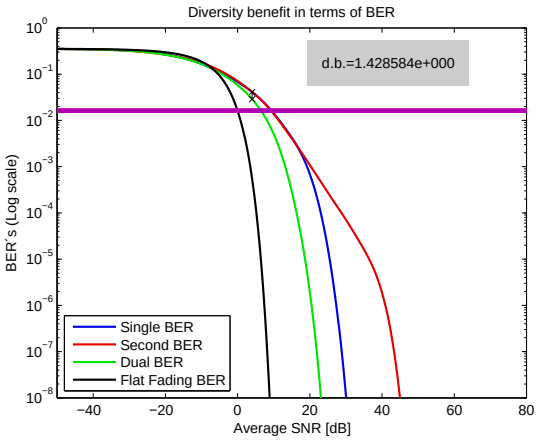

Figure 6.22: Normalized BER curves for the scenario 5 test 1, Stand/Sit/Stand

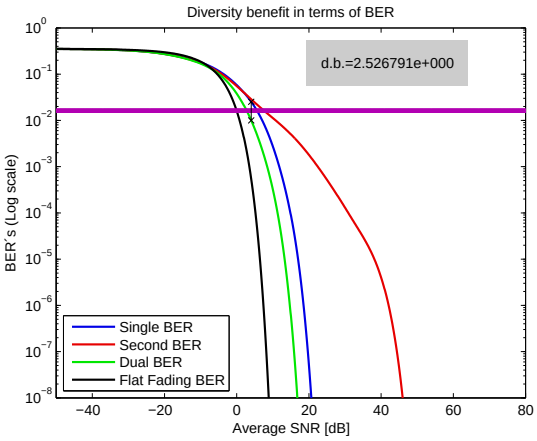

Figure 6.23: Normalized BER curves for the scenario 5 test 2, Stand/Sit/Stand

Walking

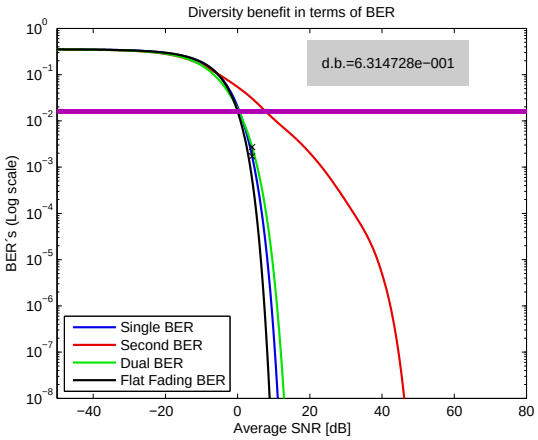

Figure 6.24: Normalized BER curves for the scenario 1 test 1,Walking

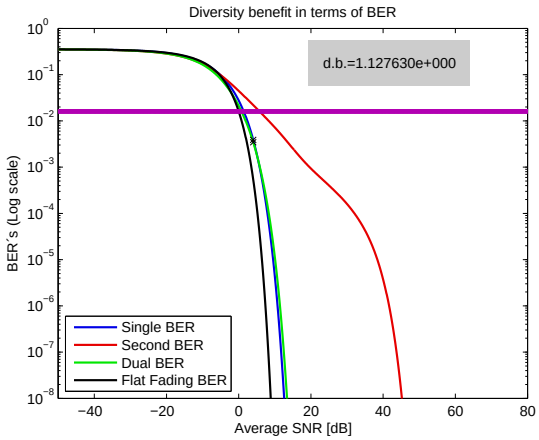

Figure 6.25: Normalized BER curves for the scenario 1 test 2, Walking

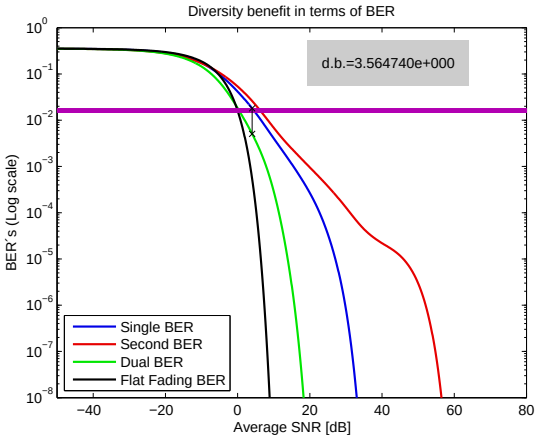

Figure 6.26: Normalized BER curves for the scenario 2 test 1, Walking

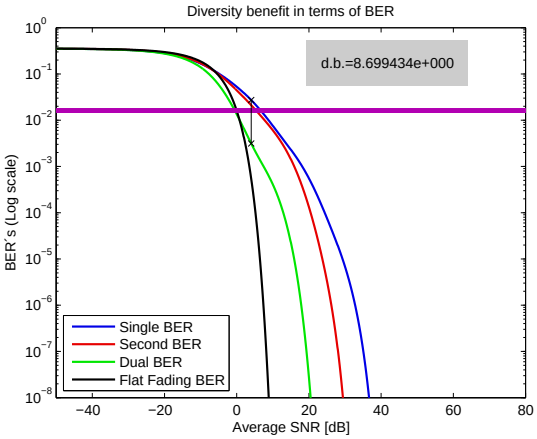

Figure 6.27: Normalized BER curves for the scenario 2 test 2, Walking

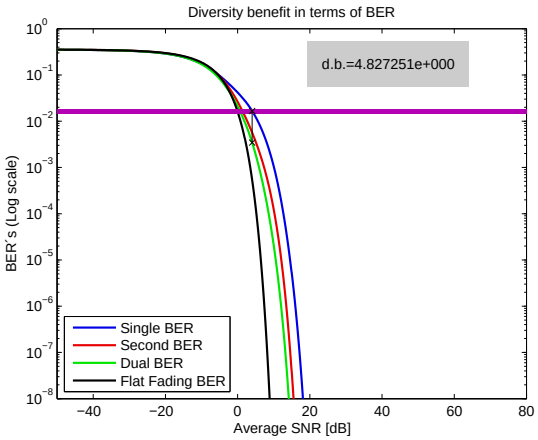

Figure 6.28: Normalized BER curves for the scenario 3 test 1, Walking

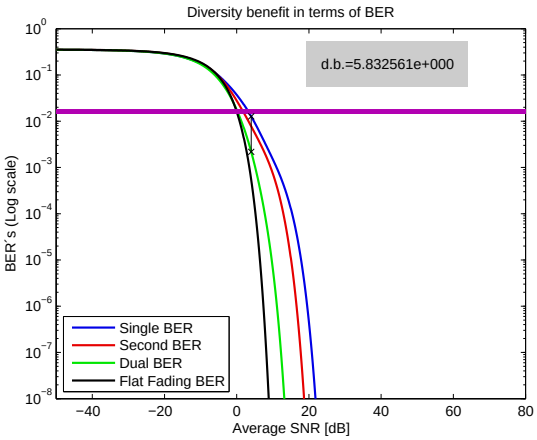

Figure 6.29: Normalized BER curves for the scenario 3 test 2, Walking

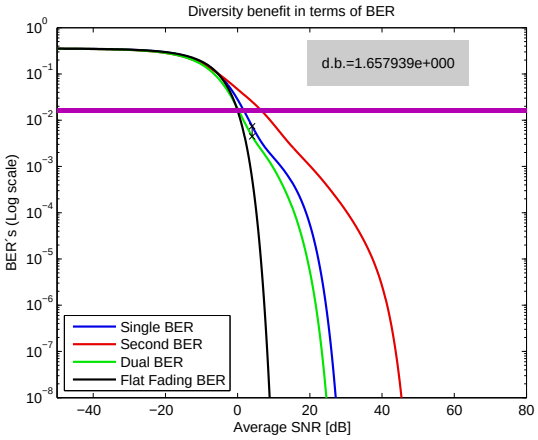

Figure 6.30: Normalized BER curves for the scenario 4 test 1, Walking

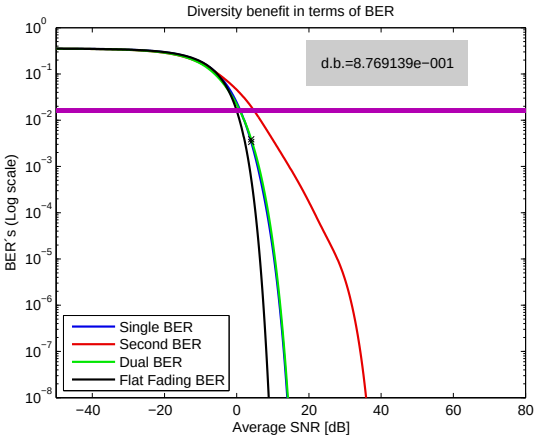

Figure 6.31: Normalized BER curves for the scenario 4 test 2, Walking

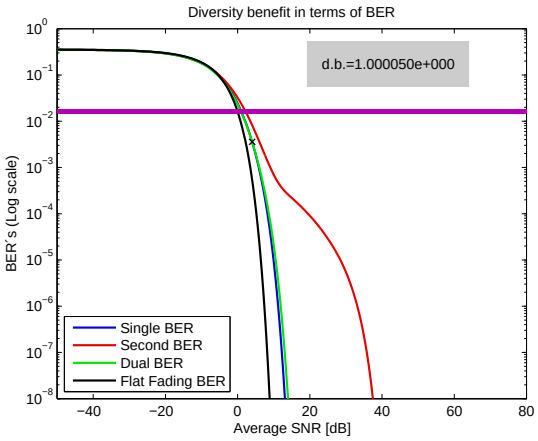

Figure 6.32: Normalized BER curves for the scenario 5 test 1, Walking

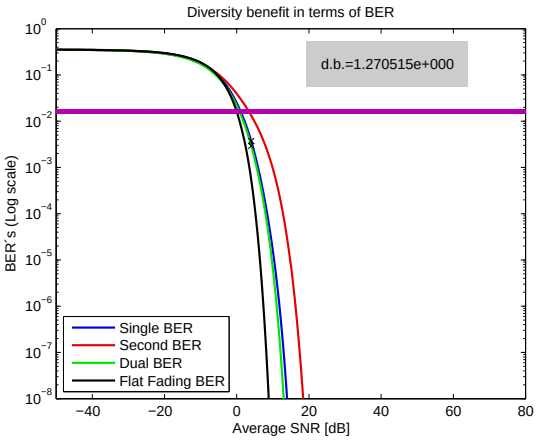

Figure 6.33: Normalized BER curves for the scenario 5 test 2, Walking